

2006

Cooperative mobile target capture using artificial potential and sliding mode control

Jingyi Yao
University of Dayton

Follow this and additional works at: https://ecommons.udayton.edu/graduate_theses

Recommended Citation

Yao, Jingyi, "Cooperative mobile target capture using artificial potential and sliding mode control" (2006).
Graduate Theses and Dissertations. 6505.
https://ecommons.udayton.edu/graduate_theses/6505

This Thesis is brought to you for free and open access by the Theses and Dissertations at eCommons. It has been accepted for inclusion in Graduate Theses and Dissertations by an authorized administrator of eCommons. For more information, please contact mschlangen1@udayton.edu, ecommons@udayton.edu.

Cooperative Mobile Target Capture Using Artificial Potential
and Sliding Mode Control

A Thesis

Submitted to

The School of Engineering of the
UNIVERSITY OF DAYTON

In Partial Fulfillment of the Requirements for
The Degree

Master of Science in Electrical Engineering

by

Jingyi Yao

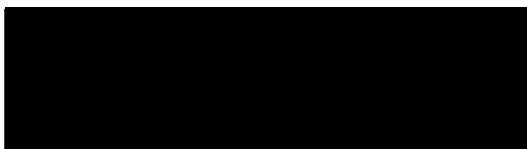
UNIVERSITY OF DAYTON

Dayton, Ohio

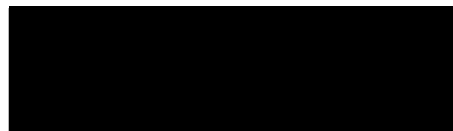
August, 2006

Cooperative Mobile Target Capture Using Artificial Potential and Sliding Mode Control

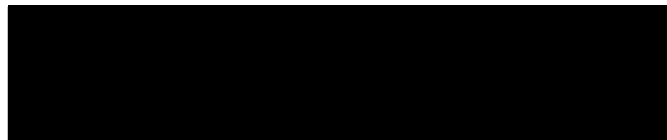
APPROVED BY:



Raúl Ordóñez, Ph.D.
Advisory Committee Chairman
Associate Professor
Department of Electrical and
Computer Engineering



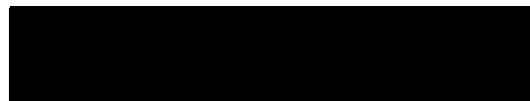
John S. Loomis, Ph.D.
Committee Member
Associate Professor
Department of Electrical and
Computer Engineering



Russell C. Hardie, Ph.D.
Committee Member
Professor
Department of Electrical and Computer Engineering



Donald L. Moon, Ph.D.
Associate Dean
Graduate Engineering Program &
Research, School of Engineering



Joseph E. Saliba, Ph.D., P.E.
Dean, School of Engineering

To my parents and friends.

ACKNOWLEDGMENTS

This Thesis is by far the most significant academic accomplishment in my life and it would be impossible without people who supported me and believed in me.

My foremost thank goes to my advisor Professor Raúl Ordóñez. I thank him for his patience and encouragement that carried me on through the master program, and for his insights and suggestions that helped to shape my research skills. Without his support, this dissertation would not have been possible. I appreciate his passion in control, academic attitude and pleasant personality. I am really glad that I got to know professor Ordóñez in my life.

This work would not have been possible without the help from Professor Veyssel Gazi at TOBB University of Economics and Technology, Turkey. He's such a warmhearted person always being there to answer any of my questions. My research benefits a lot from detailed discussion with him and his valuable feedback contributed greatly to my work. I would also like to thank Professor John Loomis, Professor Russel Hardie for serving in my thesis committee and helping me to improve this thesis.

Moreover, I want to thank research colleagues in the Control Group: Chunlei Zhang, Schreecha- ran Kanchanavally, Kayode Ajayi-Majebi, Sangeetha Sangameswaran and Sangameshwar Sonth, for their valuable discussions and suggestions, and in general creating a nice environment to be in and perform research.

Finally, I would like to thank my parents for their deep love and confidence in me, thank all my friends encouraging and supporting me in my life and study, helping me go through my tough time. The thesis is dedicated to them.

ABSTRACT

This thesis presents a stable and decentralized control strategy to the problem of controlling multi-agent systems (swarms) capturing a moving target while maintaining a desired formation. The coordination framework uses artificial potentials specifying desired distances between pairs of agents to take care of both tracking and formation tasks. The problem is actually an optimization problem and our purpose is to design a controller to minimize potential function. The controller design procedure consists of two stages. The first stage is the definition of an appropriate sliding manifold. In Chapter2, we consider agents in “kinematic” model and develop a controller for that case. Actually, we defined a sliding surface for the general dynamic model in Chapter3 at the same time. The second stage of the sliding mode control design is to enforce occurrence of sliding mode on the assigned surface and this was discussed in Chapter3. The algorithm is robust with respect to the system uncertainties and additive disturbances. Finally, given specific potential functions, simulation results following the designed control law are shown in order to illustrate the procedure.

TABLE OF CONTENTS

	Page
Abstract	v
List of Figures	viii
Chapters:	
1. Introduction	1
1.1 Motivation	1
1.2 Literature Overview	2
1.3 Thesis Outline	5
1.4 Contribution	6
2. Basic “Kinematic Model”	7
2.1 Problem Statement	7
2.2 Artificial Potential	8
2.2.1 Potential for Tracking	9
2.2.2 Potential for Formation	10
2.3 Controller Design	13
2.4 Extended Discussion	15
3. Sliding Mode Control for Agents with Vehicle Dynamics	19
3.1 Mathematic Model	19
3.2 Cooperative Tracking via Sliding Mode	20
3.3 Low Pass Filter	23
4. Results: Simulation	26
4.1 Potential function with a unique minimum	26
4.2 Potential function with local minima	30
4.3 Formation switching	33

5. Conclusions	43
Bibliography	45

LIST OF FIGURES

Figure	Page
2.1 Distributed Control for Swarm.	8
2.2 Example of Potential Function: $\delta_{it} = 1$. (a) J . (b) $\text{Grad}(J)$	10
2.3 Example of Potential Function: $\delta_{ij} = 0.7$. (a) J . (b) $\text{Grad}(J)$	11
3.1 Lowpass filter ($\mu = 0.1$).	24
4.1 Formation graph for 4 agents and target: $a = 1, b = 2, c = \sqrt{3}$	28
4.2 Formation graph for 6 agents and target: $a = 1/\sqrt{3}, b = 2/\sqrt{3}, c = 1$	29
4.3 Swarm performance for $N = 4$ using potential function with unique minimum. (a) The paths of the swarm members. (b) Zoomed out final position of the swarm. (c) Distance between agent and target. (d) Distance between agents. (e) Formation keeping. (f) Potential function.	35
4.4 Swarm performance for $N = 6$ using potential function with unique minimum. (a) The paths of the swarm members. (b) Zoomed out final position of the swarm. (c) Distance between agent and target. (d) Distance between agents. (e) Formation keeping. (f) Potential function.	36
4.5 Swarm performance for $N = 4$ using potential function with local minima. (a) The paths of the swarm members. (b) Zoomed out final position of the swarm. (c) Distance between agent and target. (d) Distance between agents. (e) Formation keeping. (f) Potential function.	37
4.6 Swarm performance for $N = 6$ using potential function with local minima. (a) The paths of the swarm members. (b) Zoomed out final position of the swarm. (c) Distance between agent and target. (d) Distance between agents. (e) Formation keeping. (f) Potential function.	38

4.7	Swarm performance for $N = 4$ using improved potential function with local minima. (a) The paths of the swarm members. (b) Zoomed out final position of the swarm. (c) Distance between agent and target. (d) Distance between agents. (e) Formation keeping. (f) Potential function.	39
4.8	Swarm performance for $N = 6$ using improved potential function with local minima. (a) The paths of the swarm members. (b) Zoomed out final position of the swarm. (c) Distance between agent and target. (d) Distance between agents. (e) Formation keeping. (f) Potential function.	40
4.9	Swarm performance ($N = 4$) of formation switching at $t = 10$. (a) The paths of the swarm members. (b) Formation changing. (c) Distance between agent and target. (d) Distance between agents.	41
4.10	Swarm performance ($N = 4$) of time-varying formation. (a) The paths of the swarm members. (b) Formation changing. (c) Distance between agent and target. (d) Distance between agents.	42

CHAPTER 1

INTRODUCTION

1.1 Motivation

In recent years it has become popular to study the biological world and apply the derived principles to the design of engineering. In nature, formation behaviors, like flocking and schooling, benefit the animals that use them in various ways. Each animal in a herd, for instance, benefits by minimizing its encounters with predators. By grouping, animals also combine their sensors to maximize the chance of detecting predators or to more efficiently forage for food. Studies of flocking and schooling show that these behaviors emerge as a combination of a desire to stay in the group and yet simultaneously keep a separation distance from other members of the group. Since groups of artificial agents could similarly benefit from formation tactics, the topic of distributed coordination and control of multiple autonomous agents has gained lots of attention. People have drawn from these biological studies to develop formation behaviors for both simulated agents and robots. Cooperative agents can often be used to perform tasks that are too difficult for a single one to perform. In addition, there are greater flexibility and adaptability of the system to the environment, robustness to failures among others.

The problem of coordination and control of multiple autonomous agents is of critical importance for military, as well as civilian applications. In the military context, engineering swarm applications include cooperative search by multiple agents, control of satellite formations or clusters of telescopes, undersea or deep space exploratory missions. The research of capabilities for integration of uninhabited air vehicles (UAVs) in the military force has been selected as one of the top priorities of the USAF. Within the civilian context, possible applications of such systems include automated highways, air traffic control, coordinated control of vehicles involved in search and rescue operations, cooperative control of mobile robots capable of navigating and inspecting dangerous areas with lower cost.

The cooperative mobile target capture problem is one of the engineering swarm applications. Instead of the traditional trajectory tracking problem, researchers began to study coordinated tracking. *The research work in this thesis is finding a coordinated control scheme for a group of agents to make them achieve and maintain some given geometrical formation and track a target or a trajectory at the same time. Each agent has global knowledge of the team configuration but is unaware of the other agents' desired destinations.*

1.2 Literature Overview

Formation control is one of the popular sub-problems of multi-agent coordination. In [1], controller was designed to keep multiple vehicles in a required formation which is treated as a single entity and classical feedback design algorithm is used to force the robots embedded in such a rigid structure. In [2], a behavior based formation control of multiple land robots integrated with the other navigational goals of the robots is described. In [3, 4], Kumar and his coworkers used graph theory to model a formation of robots navigating a terrain with obstacles. In [5], Olfati-Saber and

Murray developed a formation control strategy by using concepts from graph theory and Lyapunov theory. In [6], Lawton and his colleagues considered nonholonomic robots and developed a strategy based on decomposing complex formation maneuvers into a sequence of maneuvers between formation patterns. The results in [7, 8] done by Leonard and coworkers, on the other hand, are based on using virtual leaders and artificial potentials for vehicle interactions in a group of agents for maintenance of the group geometry. They used the system kinetic energy and the artificial potential energy as a Lyapunov function to prove closed loop stability and employed a dissipative term to achieve asymptotic stability of the formation. Egerstedt [9] also developed a formation control strategy based on formation functions and virtual leaders and verified the algorithm by applying it to a kinematic model of mobile robots. In [10, 11, 12], Veysel and Kevin have done extensive work on swarm stability and introduce an attractant/repellent profile (i.e., a profile of nutrients or toxic substances) to model the environment. Potential function and sliding mode control method have been successfully used to implement engineering aggregating swarm and tracking moving target in [13, 14]. The research reported in this thesis benefits from these two papers and could be regarded as an extension of them.

Although formation control is approached in different ways with various analysis techniques, the strategies can be categorized to three main architectures: (i) *Multi-input Multiple-output*, in which the formation is treated as a single multiple-input, multiple-output plant, (ii) *Leader-follower*, in which individual agent controllers are connected hierarchically, (iii) *Cyclic*, in which individual agent controllers are connected non-hierarchically. [15]. The strategy used by works introduced above is based on either one of them or the combination.

The *MIMO* architecture has highest optimality and stability, but is not robust to local failures because controller is centralized. The *L/F* architecture reduces formation control to individual tracking problems, each agent only needs information about its leaders. This fact simplifies formation coordination. However, because only leaders are set to perform the tracking task without considering the followers, once the leader fails, the whole task would also fail. The *Cyclic* architecture lies between the *MIMO* and *L/F* architectures. By allowing non-hierarchical connections between individual agent controllers, cyclic algorithms can be completely decentralized in the sense that there is neither a coordinating agent (leader) nor instability resulting from single point failures. Therefore, *we build our strategy based on Cyclic architecture*. Generally, potential field-based cyclic algorithms have a stability proof since the potential function itself serves as the basis for a Lyapunov function. *The research work in this thesis uses artificial potentials and sliding mode technique, with classic control tools (such as Lyapunov or LaSalle theorems) for proving the swarm behavior.*

The concept of *artificial potential function* is not new, and it has been used extensively for robot navigation and control [16, 17]. Most recently, the studies have extended potential field methods to the maneuvering of group behaviors such as formation, migration and obstacle avoidance in swarm system [18, 7, 13, 14]. The artificial potential function is created to encode the interaction rule for the group and model the environment. In order to perform the tasks of formation control and target tracking, we consider a potential function composed of two parts. The interconnection part defines social rule for the group, making the agent constrained by its neighbor to maintain a group structure. This part includes functions of the relative distance between each pair of neighbors. In addition, pursuer-target potential function is introduced to direct the group behavior, which is to catch up with the target. Then the combination of the two rules will fulfill the overall goal. The specific

form of potential function is defined according to the desired geometric formation. A fundamental problem in the application of potential field method is how to deal with the local minima [19]. How to construct a potential function is important because different potentials might result in different performance even with the same control algorithm. In particular, existence of multiple local minima in the potential function leads to guaranteeing only local convergence to the desired formation. Nevertheless, we show that by appropriate choice of the potential function one can always guarantee that eventually the target will be surrounded or “enclosed” by the tracking agents.

The *sliding mode control technique* is a approach to robust control and has the important properties of suppressing disturbances and model uncertainties. It becomes attractive for two main advantages: (i) the dynamic behavior of the system may be tailored by the particular choice of switching function, and (ii) the closed-loop response becomes totally insensitive to a particular class of uncertainties. In [20, 21], it is used for robot navigation and obstacle avoidance in an environment modeled with harmonic potentials. In [13, 14], it has shown that this method can be used for implementation formation control as well as target tracking. Similarly, we use this technique to force the motion of the agent along the required behavior.

1.3 Thesis Outline

The thesis is organized as follows: In Chapter 2, we begin with the formulation of our research problem: networked agents cooperatively tracking mobile target in a required formation. A simple mathematical model defined as “kinematic” model is proposed for agents in the group. After introducing a general potential function with proper assumptions, a control algorithm is developed and the proving is given using classic control tool Lyapunov/LaSalle principles. Basic results are gained and discussed here which can serve as guidelines for next step designing. In Chapter 3,

we consider a general fully actuated dynamic model of the agents and derive a new controller based on the sliding mode control method. The results in the preceding chapter are recovered. In Chapter 4, we show several simulation results of cooperative mobile target capture in different formations. Specific potential functions are applied to the problem and results are presented and discussed. Finally, conclusions are made in Chapter 5. The main chapters in this thesis are essentially from the conference paper [22].

1.4 Contribution

As we have stated above, much significant work has been reported on the topic of distributed coordination and control of multiple autonomous agents. Many different approaches are proposed and demonstrated so far. But each one has its advantage and disadvantage, or with several unresolved technical problems. The research in this thesis has the following advantages comparing to others. First, all of the recent investigations have been limited to either one or two-dimensional space, our work generally applies to n -dimensional. Second, artificial potential function approach make it easy for swarm to include the collision avoidance task, and possible to track a wider class of target instead of constant or periodic trajectories. Third, while results of some papers are restricted to one particular swarm model, the procedure based on sliding mode control is more general and can be used for other similar models using artificial potentials. Also, sliding mode technique enables the achievement of tasks despite model uncertainties.

CHAPTER 2

BASIC “KINEMATIC MODEL”

2.1 Problem Statement

Consider a multi-agent system (i.e., a swarm) consisting of N individuals in an n -dimensional Euclidean space. Our objective is to make the entire group (N agents) catch and aggregate around the target and move together with it possibly in a specific formation regardless of the target’s movement. This is a simple case of the coordinated tracking problem. There are two tasks involved: target tracking and formation control.

To begin with, we model the individuals as points and ignore their dimensions. Moreover, we assume synchronous motion and no time delays. Let $x_i, x_t \in \mathbb{R}^n$ denote the position vector of individual i and the target respectively. In this chapter, we assume that the motion dynamics for the agents are given by

$$\dot{x}_i = u_i \tag{2.1}$$

which we call the “kinematic model”. $u^i \in \mathbb{R}^n$ is the control input for the i^{th} agent. We will show how the derivations in this chapter can be extended to the case in which the agents have fully actuated dynamics in next chapter.

Different from the traditional problem, which is either regulation or tracking, the problem here is tuned to be an optimization problem by using artificial potentials.

The potential function is actually a performance function, which has only one unique global minimum — the goal configuration. It can be measured by the agents. Our purpose is to construct a potential function J according to our goal (here we want each agent to reach the desired distance from target and other agents) and then design a control law for each agent to minimize J to that global minimum, implying the achievement of target capture and formation control. A block diagram can be found in Figure 2.1.

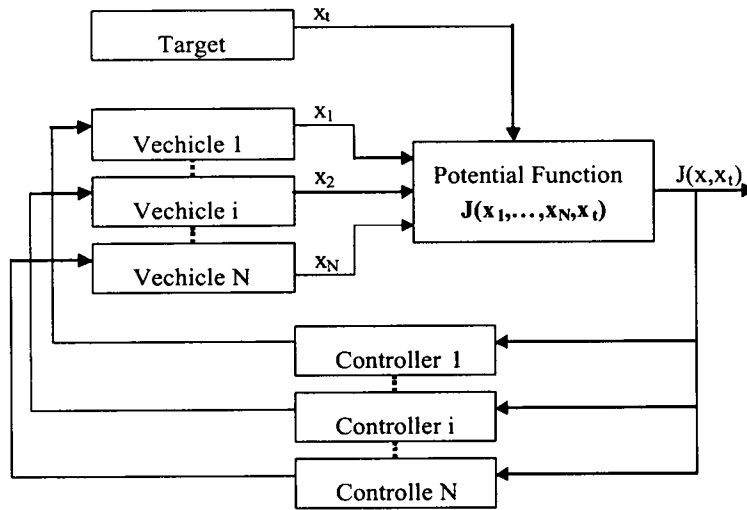


Figure 2.1: Distributed Control for Swarm.

2.2 Artificial Potential

Let's construct a potential function generally. In order to satisfy both the tracking and formation control specifications, potential functions $J(x, x_t)$ are constructed such that they are composed of two parts - the agent-target interaction (or tracking) part and the inter-agent interactions (or formation control) part. In particular, we consider

potential functions of the form

$$J(x, x_t) = K_T \sum_{i=1}^N J_{it}(\|x_i - x_t\|) + K_F \sum_{i=1}^{N-1} \sum_{j=i+1}^N J_{ij}(\|x_i - x_j\|) \quad (2.2)$$

where $J_{it}(\|x_i - x_t\|)$ is the potential between agent and target, while $J_{ij}(\|x_i - x_j\|)$ is the potential between agents in the group. The coefficients K_T and K_F weigh the relative importance of tracking versus formation keeping. With such a form, each agent has to know the relative distances from target and from other agents, so that it can take care of the tracking task by itself and keeps certain distances between itself and its neighbors. Note also that in the above equation we implicitly defined $x^\top = [x_1^\top, \dots, x_N^\top] \in \mathbb{R}^{n \times N}$.

2.2.1 Potential for Tracking

First, consider the potential for tracking part

$$J_T(x, x_t) = \sum_{i=1}^N J_{it}(\|x_i - x_t\|) \quad (2.3)$$

It is required that $J_{it}(\|x_i - x_t\|)$ has a unique minimum when the individual catches up with the target by a prescribed distance without collision, which means

$$\nabla_{x_i} J_{it}(\|x_i - x_t\|) = 0 \text{ if and only if } \|x^i - x^t\| = \delta_{it} \quad (2.4)$$

Let's assume $J_{it}(\|x_i - x_t\|)$ satisfies:

(A1) There exist corresponding function $h^{it} : \mathbb{R}^+ \rightarrow \mathbb{R}$ such that

$$\nabla_y J_{it}(\|y\|) = y h^{it}(\|y\|) \quad (2.5)$$

(A2) There exist unique distances δ_{it} at which we have $h^{it}(\|y\|) = 0$.

Figure 2.2 is an example of a potential function which satisfied these assumptions, where $J_y(\|y\|) = \frac{1}{2}(\|y\|^2 - \delta_{it}^2)^2$. It is a one-dimensional case.

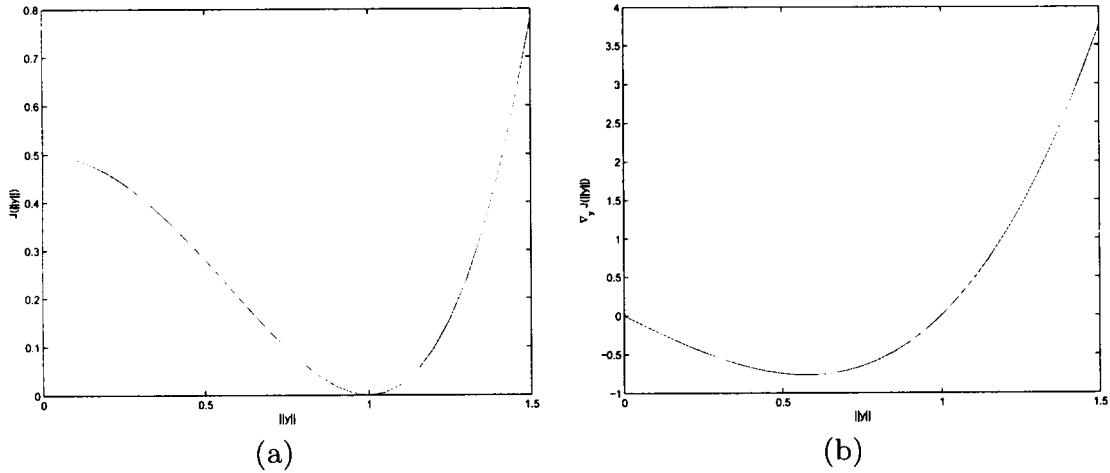


Figure 2.2: Example of Potential Function: $\delta_{it} = 1$. (a) J . (b) $\text{Grad}(J)$.

2.2.2 Potential for Formation

Second, consider the potential for formation part, which governs inter-agent relationship that applied locally, a team of agents can exhibit collision-free formation maintenance.

$$J_F(x, x_t) = \sum_{i=1}^{N-1} \sum_{j=i+1}^N J_{ij}(\|x_i - x_j\|) \quad (2.6)$$

$J_{ij}(\|x_i - x_j\|)$ is the potential between i^{th} and j^{th} agent and is required to have a unique minimum at the desired distance between them, based on the formation expected to be achieved. Note that $J_{ij}(\|x_i - x_j\|)$ can be different for different pairs. (The same could be the case for $J_{it}(\|x_i - x_t\|)$ as well although we used the same $J_{it}(\|x_i - x_t\|)$ for all i here.)

Let's assume $J_{ij}(\|x_i - x_j\|)$ satisfies:

(B1) The potentials $J_{ij}(\|x_i - x_j\|)$ are symmetric and satisfy

$$\nabla_{x_i} J_{ij}(\|x_i - x_j\|) = -\nabla_{x_j} J_{ij}(\|x_i - x_j\|) \quad (2.7)$$

(B2) There exist corresponding function $g^{ij} : \mathbb{R}^+ \rightarrow \mathbb{R}$ such that

$$\nabla_y J_{ij}(\|y\|) = yg^{ij}(\|y\|) \quad (2.8)$$

(B3) There exist unique distances δ_{ij} at which we have

$$g^{ij}(\|y\|) = \begin{cases} > 0, & \|y\| > \delta_{ij} \\ = 0, & \|y\| = \delta_{ij} \\ < 0, & \|y\| < \delta_{ij} \end{cases}$$

Potential functions satisfying these conditions are odd functions that are attractive on distances $\|y\| > \delta_{ij}$ and repulsive on distances $\|y\| < \delta_{ij}$. The term $g^{ij}(\|y\|)$ determines the attraction-repulsion relationship between the individuals. The distance δ_{ij} is the equilibrium distance at which the attraction and the repulsion balance. That is, the potential function $J_{ij}(\|x^i - x^j\|)$ has a minimum at $\|x^i - x^j\| = \delta_{ij}$. Given a potential function J_F encoding a desired formation, the formation control will be realized if J_{ij} for all N is minimized.

Figure 2.3 is an example of a potential function which meets these assumptions, where $J_y(\|y\|) = \frac{a}{2}\|y\|^2 + \frac{bc}{2}\exp(-\frac{\|y\|^2}{c})$ with $a = 1.7259, b = 20, c = 0.2$. It is also a one-dimensional case.

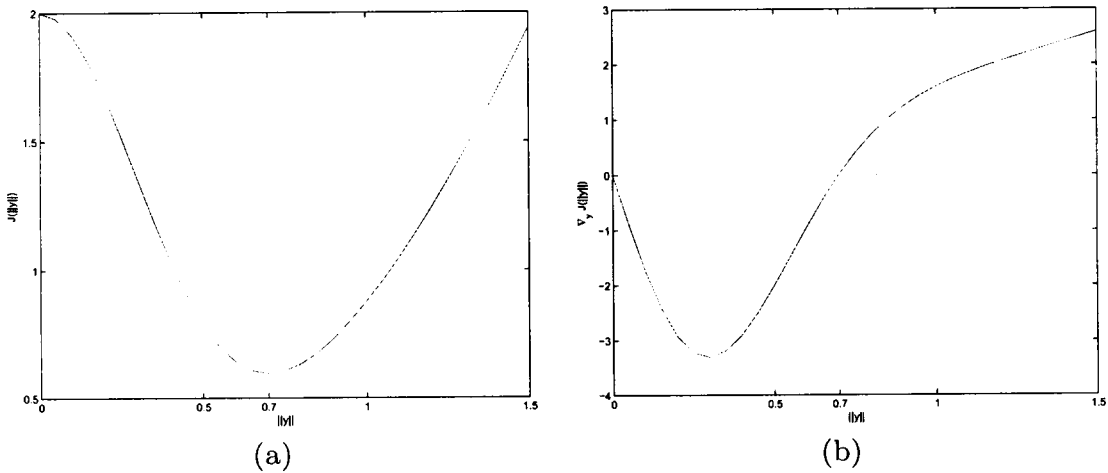


Figure 2.3: Example of Potential Function: $\delta_{ij} = 0.7$. (a) J . (b) $\text{Grad}(J)$.

Definition (Potential function): $J : \mathbb{R}^{n \times N} \times \mathbb{R}^n \rightarrow \mathbb{R}$ is a differentiable, nonnegative, decrescent, radially unbounded function of the distance $\|x_i - x_t\|$ between agent i and target, and the distance $\|x_i - x_j\|$ between agent i and j , such that

- J has only one minimum and attains its unique minimum when $\|x_i - x_t\| = \delta_{it}$ and $\|x_i - x_j\| = \delta_{ij}$ for all i and j ($i, j = 1, \dots, N$).
- $\nabla_{x_t} J(x, x_t) = - \sum_{i=1}^N \nabla_{x_i} J(x, x_t)$.

The potential function defined in (2.2) is based on relative positions instead of absolute positions. Hence, J has one minimum for symmetrical formation as well, considering translation and rotation of all the agents and target. The definition ensures that minimization of the function implies desired formation of agents and target.

The second term in definition is an important relationship based on all the assumptions made about the potential function. It will be used in the proof in next section.

Take partial derivative of $J(x, x_t)$, we have

$$\begin{aligned} \nabla_{x_i} J(x, x_t) &= K_T (x_i - x_t) h^{it} (\|x_i - x_t\|) \\ &+ K_F \sum_{j=1, j \neq i}^N (x_i - x_j) g^{ij} (\|x_i - x_j\|) \end{aligned} \quad (2.9)$$

$$\nabla_{x_t} J(x, x_t) = -K_T \sum_{i=1}^N (x_i - x_t) h^{it} (\|x_i - x_t\|) \quad (2.10)$$

By observing the equalities in (2.9) and (2.10), the equality in (2.10) can be rewritten as

$$\begin{aligned} \nabla_{x_t} J(x, x_t) &= - \sum_{i=1}^N \nabla_{x_i} J(x, x_t) \\ &+ K_F \sum_{i=1}^N \sum_{j=1, j \neq i}^N (x_i - x_j) g^{ij} (\|x_i - x_j\|) \end{aligned} \quad (2.11)$$

Moreover, since we have

$$\sum_{i=1}^N \sum_{j=1, j \neq i}^N (x_i - x_j) g^{ij}(\|x_i - x_j\|) = 0 \quad (2.12)$$

which follows from (2.7), we then obtain the useful relationship:

$$\nabla_{x_t} J(x, x_t) = - \sum_{i=1}^N \nabla_{x_i} J(x, x_t) \quad (2.13)$$

2.3 Controller Design

Based on the definition we made for Potential Function, it also serves as Lyapunov Function for stability proof. It is specified by the multi-agent system designer based on the desired behavior of the swarm. Taking the time derivative of J and substituting the condition (2.13) in the \dot{J} equation, one obtains

$$\begin{aligned} \dot{J} &= \sum_{i=1}^N [\nabla_{x_i} J(x, x_t)]^\top \dot{x}_i + [\nabla_{x_t} J(x, x_t)]^\top \dot{x}_t \\ &= \sum_{i=1}^N [\nabla_{x_i} J(x, x_t)]^\top u_i - \sum_{i=1}^N [\nabla_{x_i} J(x, x_t)]^\top \dot{x}_t \\ &= \sum_{i=1}^N [\nabla_{x_i} J(x, x_t)]^\top (u_i - \dot{x}_t) \end{aligned} \quad (2.14)$$

We can design a controller in a simpler form if \dot{x}_t is available [14]. We could choose the control law for all agents as

$$u_i = \dot{x}_t - \alpha \nabla_{x_i} J(x, x_t) \quad (2.15)$$

for some constant $\alpha > 0$ and substitute it in the \dot{J} equation, one obtains

$$\begin{aligned} \dot{J} &= \sum_{i=1}^N [\nabla_{x_i} J(x, x_t)]^\top (u_i - \dot{x}_t) \\ &= \sum_{i=1}^N [\nabla_{x_i} J(x, x_t)]^\top (\dot{x}_t - \alpha \nabla_{x_i} J(x, x_t) - \dot{x}_t) \\ &= -\alpha \sum_{i=1}^N \|\nabla_{x_i} J(x, x_t)\|^2 \leq 0 \end{aligned} \quad (2.16)$$

However, assuming that \dot{x}_t is known is a strong assumption since the current velocity of the target is unknown in most circumstances. It is more realistic to assume that $\|\dot{x}_t\| \leq \gamma_t$ for some known $\gamma_t > 0$ since any realistic agent has a bounded velocity. We also assume that the relative position of the target x_t is known and each agent knows the exact relative positions of all the other individuals.

With the assumptions above, we choose the control law as

$$u_i = -\alpha \nabla_{x_i} J(x, x_t) - \beta \text{sign}(\nabla_{x_i} J(x, x_t)) \quad (2.17)$$

for all $i = 1, \dots, N$ where $\alpha > 0$ and $\beta \geq \gamma_t$ are positive constants, $\text{sign}(\cdot)$ is the signum function operated elementwise for a vector $y \in \mathbb{R}^n$, i.e., $\text{sign}(y) = [\text{sign}(y_1), \dots, \text{sign}(y_n)]^\top$.

Then the time derivative of function J is given by

$$\begin{aligned} \dot{J} &= \sum_{i=1}^N [\nabla_{x_i} J(x, x_t)]^\top (u_i - \dot{x}_t) \\ &= \sum_{i=1}^N [\nabla_{x_i} J(x, x_t)]^\top (-\alpha \nabla_{x_i} J(x, x_t) - \beta \text{sign}(\nabla_{x_i} J(x, x_t)) - \dot{x}_t) \\ &= -\alpha \sum_{i=1}^N \|\nabla_{x_i} J(x, x_t)\|^2 - \beta \sum_{i=1}^N \|\nabla_{x_i} J(x, x_t)\| - \sum_{i=1}^N [\nabla_{x_i} J(x, x_t)]^\top \dot{x}_t \\ &\leq -\alpha \sum_{i=1}^N \|\nabla_{x_i} J(x, x_t)\|^2 - \beta \sum_{i=1}^N \|\nabla_{x_i} J(x, x_t)\| + \gamma_t \sum_{i=1}^N \|\nabla_{x_i} J(x, x_t)\| \\ &= -\alpha \sum_{i=1}^N \|\nabla_{x_i} J(x, x_t)\|^2 - (\beta - \gamma_t) \sum_{i=1}^N \|\nabla_{x_i} J(x, x_t)\| \end{aligned} \quad (2.18)$$

Since we have $\beta \geq \gamma_t$, the time derivative of J is bounded by

$$\dot{J} \leq -\alpha \sum_{i=1}^N \|\nabla_{x_i} J(x, x_t)\|^2 \quad (2.19)$$

We get the same result as (2.16) here.

Since J and the bound of \dot{J} all depend on t , we use *Lasalle-Yoshizawa* theorem, from which we have

$$\lim_{t \rightarrow \infty} \alpha \sum_{i=1}^N \|\nabla_{x_i} J(x, x_t)\|^2 = 0$$

We can further conclude that (x, x_t) asymptotically converges to $\|\nabla_{x_i} J(x, x_t)\| = 0$. Also from (2.13) we see that we also have $\|\nabla_{x_t} J(x, x_t)\| \rightarrow 0$. In other words, as $t \rightarrow \infty$ we have $(x, x_t) \rightarrow \Omega \subset \{(x, x_t) | \dot{J} = 0\}$ where

$$\Omega = \{(x, x_t) | \nabla_{x_t} J(x, x_t) = 0, \nabla_{x_i} J(x, x_t) = 0, i = 1 \dots N\}$$

Since we assume the potential function has only one minimum, it indicates J converges to the unique global minimum, implying that the system converges to a configuration corresponding to that minimum.

The above controller requires knowledge of the position of the target and a bound on its speed as well. With the help of a switching term, it guarantees asymptotic tracking of the target. Intuitively, the signum function term allows for the detection of the changes in the direction of the motion of the target and helps redirect the vehicle in that direction.

2.4 Extended Discussion

Potential field method have been shown to be effective and powerful in solving difficult motion planning problems such as one with high degree of freedom. However, in practice, most potential functions may have multi-minima. Because of the local-minima problem, most of the potential-based methods are heuristic.

If the potential function we construct has one unique global minimum as required in definition, we will achieve our overall goals. If the potential function has multi-minima, things are like this: when the distance between any pair of objects including agents and target ($\|x_i - x_t\|$ and $\|x_i - x_j\|$) is the desired one (δ_{it} and δ_{ij}), the potential function J reaches its global minimum, which corresponds to our tracking and formation objectives. In addition, there are other feasible configurations different from the desired one, at which the potential function J achieves a local minimum. Therefore, in general, unless the initial configuration of the agents is “close enough”

to the global minimum, it might be the case that J converges to such a local minimum resulting in a different configuration.

Now, let's suppose the specific potential function we construct has multi-minima. It is concluded above that N agents with dynamics (2.1), each steered by control law (2.17), we have

$$(x, x_t) \rightarrow \Omega = \{(x, x_t) | \nabla_{x_t} J(x, x_t) = 0, \nabla_{x_i} J(x, x_t) = 0, i = 1 \dots N\}$$

From (2.10) we have (x, x_t) in Ω satisfy

$$-K_T \sum_{i=1}^N (x_i - x_t) h^{it}(\|x_i - x_t\|) = 0$$

Rearranging this equation, we obtain

$$\sum_{i=1}^N x_i h^{it}(\|x_i - x_t\|) = x_t \sum_{i=1}^N h^{it}(\|x_i - x_t\|) \quad (2.20)$$

which is guaranteed to be achieved as $t \rightarrow \infty$. This is an important observation because it provides a relation of the position of the target to the position of the agents at equilibrium and allows the designer to appropriately choose the $h^{it}(\|x_i - x_t\|)$ (the tracking part of the potential function).

Actually, Ω can be written as $\Omega = \Omega_1 \cup \Omega_2$ where

$$\Omega_1 = \{(x, x_t) | \sum_{i=1}^N x_i h^{it}(\|x_i - x_t\|) = x_t \sum_{i=1}^N h^{it}(\|x_i - x_t\|), h^{it}(\|x_i - x_t\|) = 0, i = 1 \dots N\}$$

$$\Omega_2 = \{(x, x_t) | x_t = \frac{\sum_{i=1}^N x_i h^{it}(\|x_i - x_t\|)}{\sum_{i=1}^N h^{it}(\|x_i - x_t\|)}, h^{it}(\|x_i - x_t\|) \neq 0, i = 1 \dots N\}$$

First of all note that at the desired formation, since $\|x_i - x_t\| = \delta_{it}$ for all i , we have $h^{it}(\|x_i - x_t\|) = 0$ for all i and (2.20) is satisfied. If the initial configuration of the agents is "close" to the desired formation, $(x, x_t) \rightarrow \Omega_1$. In this case, agents catch up with the target and compose the expected formation with it.

Second issue to note is that if $(x, x_t) \rightarrow \Omega_2$ which corresponds to local minima, we can modify $h^{it}(\|y\|)$ to avoid the worst case, that is, target escape from the group.

Defining

$$\eta_i = \frac{h^{it}(\|x_i - x_t\|)}{\sum_{i=1}^N h^{it}(\|x_i - x_t\|)}, i = 1, \dots, N,$$

we obtain

$$x_t = \sum_{i=1}^N \eta_i x_i$$

With the choice of $h^{it}(\|y\|) \geq 0$ or $h^{it}(\|y\|) \leq 0$ for all y we see that $0 \leq \eta_i \leq 1$ for all i and $\sum_{i=1}^N \eta_i = 1$ implying that as $t \rightarrow \infty$ we will have $x_t \rightarrow \text{conv}\{x_1, x_2, \dots, x_N\}$, where $\text{conv}\{x_1, x_2, \dots, x_N\}$ is the convex hull of the positions of the agents. In other words, by choosing $h^{it}(\|y\|)$ as above one can guarantee that as $t \rightarrow \infty$ the agents will “surround” or “enclose” the target, which is an important result.

Despite the beauty of the above results there is one shortcoming, which is that the model in (2.1) does not represent the dynamics of realistic agents. As was discussed in [12] it is possible to argue that in some cases it can be viewed as an approximation of the point mass dynamics described by

$$\begin{aligned} \dot{x}_i &= v_i \\ m_i \dot{v}_i &= -k_v v_i + u_i \end{aligned} \tag{2.21}$$

where $-k_v v_i$ is a velocity damping term, and u_i is the control acting on agent i . This is possible for the cases in which m_i is very small ($m_i \approx 0$) and the viscosity of the environment is high (as is the case for some bacteria) which allows one to ignore m_i . Then setting $m_i = 0$ and taking $k_v = 1$ one can see that (2.21) reduces to (2.1).

Although here we are not concerned with the motion of bacteria and (2.1) does not correspond to the dynamics of realistic agents, the results derived are still of interest since they serve as proof of concept for the behavior considered. Although they do not specify how that desired behavior could be achieved in engineering applications with given agent dynamics, they can serve as guidelines for designing such applications.

In the next chapter, we discuss a control algorithm based on sliding mode control theory which could be applied for agents with general fully actuated dynamics (such as omni-directional robots).

CHAPTER 3

SLIDING MODE CONTROL FOR AGENTS WITH VEHICLE DYNAMICS

In last chapter we show that for a multi-agent system with a target (with position x_t), the group will eventually capture/enclose the target provided that the controller for each agent in “Kinematic” Model is chosen such as to satisfy Eq. (2.17). In this chapter, we will build on these results by considering the pursuing agent with realistic vehicle dynamics.

3.1 Mathematic Model

Consider all the agents in the system have the same dynamics, which could be described by the equation

$$M(x_i)\ddot{x}_i + f_i(x_i, \dot{x}_i) = u_i \quad (3.1)$$

where $x_i \in \mathbb{R}^n$ is the position of the agent, $M(x_i) \in \mathbb{R}^{n \times n}$ is the mass or inertia matrix, and $u_i \in \mathbb{R}^n$ represents the control inputs (forces). The function $f_i(x_i, \dot{x}_i) \in \mathbb{R}^n$ represents centripetal forces, Coriolis, gravitational affects and additive disturbances. For this term we assume that

$$f_i(x_i, \dot{x}_i) = f_i^k(x_i, \dot{x}_i) + f_i^u(x_i, \dot{x}_i)$$

where $f_i^k(\cdot, \cdot)$ represents the known part and $f_i^u(\cdot, \cdot)$ represents the unknown part. For the unknown part, we assume that $\|f_i^u(x_i, \dot{x}_i)\| \leq \bar{f}_i$, where $\bar{f}_i < \infty$ is a known

constant. Moreover, it is assumed that for all x_i the matrix $M(x_i)$ satisfies

$$\underline{M}\|y\|^2 \leq y^\top M(x_i)y \leq \overline{M}\|y\|^2$$

where \underline{M} and \overline{M} are known and $y \in \mathbb{R}^n$ is arbitrary. Note that all these assumptions are standard and realistic.

This model for motion dynamics of the agents is more general than those in [7, 8]. Moreover, it allows for possible additive disturbances (which are not included in [7, 8]). This advantage is basically due to the robustness properties of the technique we are going to use — the sliding mode algorithm.

3.2 Cooperative Tracking via Sliding Mode

Given the dynamics above, we would like to choose the control input u_i such that as time progresses the agents catch the target in a formation. In order to achieve this objective, there might be several different approaches. The approach we are going to take in this chapter is to enforce the velocity of the agent to satisfy Eq. (2.17). In other words, if the control input is designed to enforce the velocity of the agent to satisfy Eq. (2.17), then the discussion in the preceding chapter guarantees that the group catches up with the target, or at least encloses it, and achieves the desired formation.

Here, we will use the sliding mode control method. Sliding mode control technique has the property of reducing the motion (and the analysis) of a system's dynamics to a lower dimensional space, which makes it very suitable for this application. We will follow a procedure similar to that in [13, 14] for swarm aggregation and single pursuer-target tracking.

Define the n -dimensional sliding manifold for agent i as

$$s_i = \dot{x}_i + \alpha \nabla_{x_i} J(x, x_t) + \beta \text{sign}(\nabla_{x_i} J(x, x_t)) \quad (3.2)$$

Note that once the agent reaches its sliding manifold (i.e., once $s_i = 0$), we have

$$\dot{x}_i = -\alpha \nabla_{x_i} J(x, x_t) - \beta \text{sign}(\nabla_{x_i} J(x, x_t)) \quad (3.3)$$

which is exactly the motion equation in last chapter. Now, let's design the control input u_i to enforce the occurrence of sliding mode. A sufficient condition for sliding mode to occur is given by

$$s_i^\top \dot{s}_i < 0 \quad (3.4)$$

which also guarantees that the sliding manifold is asymptotically reached.

Differentiating the sliding manifold equation we obtain

$$\dot{s}_i = \ddot{x}_i + \frac{\partial}{\partial t} [\alpha \nabla_{x_i} J(x, x_t)] + \frac{\partial}{\partial t} [\beta \text{sign}(\nabla_{x_i} J(x, x_t))] \quad (3.5)$$

Let us assume for now that $\|\frac{\partial}{\partial t} [\beta \text{sign}(\nabla_{x_i} J(x, x_t))]\| \leq \bar{J}_s$ and $\|\frac{\partial}{\partial t} [\alpha \nabla_{x_i} J(x, x_t)]\| \leq \bar{J}$ where \bar{J}_s and \bar{J} are known positive constants. Since the potential function is to be chosen by the designer, he or she should make sure that $\|\frac{\partial}{\partial t} [\alpha \nabla_{x_i} J(x, x_t)]\| \leq \bar{J}$ is satisfied for some \bar{J} . In the next chapter we will consider potential functions which satisfy these bounds. Note also that $\|\frac{\partial}{\partial t} [\beta \text{sign}(\nabla_{x_i} J(x, x_t))]\|$ is unbounded at the instances at which $\text{sign}(\nabla_{x_i} J(x, x_t))$ changes sign. This problem will be solved by using a low pass filter and will be discussed below.

From the vehicle dynamics of the agents in Eq. (3.1), we have

$$\ddot{x}_i = M^{-1}(x_i)[u_i - f_i(x_i, \dot{x}_i)]$$

which is used in the \dot{s}_i equation and substitute it in Eq. (3.4).

By choosing

$$u_i = -u_0 \text{sign}(s_i) + f_i^k(x_i, \dot{x}_i) \quad (3.6)$$

and the gain u_0 of control input as

$$u_0 > \bar{M} \left(\frac{1}{\underline{M}} \bar{f}_i + \bar{J} + \bar{J}_s + \epsilon \right) \quad (3.7)$$

We have

$$\begin{aligned}
s_i^\top \dot{s}_i &= s_i^\top [\ddot{x}_i + \frac{\partial}{\partial t}[\alpha \nabla_{x_i} J(x, x_t)] + \frac{\partial}{\partial t}[\beta \text{sign}(\nabla_{x_i} J(x, x_t))]] \\
&= s_i^\top [M^{-1}(x_i)[u_i - f_i(x_i, \dot{x}_i)] + \frac{\partial}{\partial t}[\alpha \nabla_{x_i} J(x, x_t)] + \frac{\partial}{\partial t}[\beta \text{sign}(\nabla_{x_i} J(x, x_t))]] \\
&= s_i^\top [M^{-1}(x_i)[-u_0 \text{sign}(s_i) + f_i^k(x_i, \dot{x}_i) - f_i(x_i, \dot{x}_i)] + \\
&\quad \frac{\partial}{\partial t}[\alpha \nabla_{x_i} J(x, x_t)] + \frac{\partial}{\partial t}[\beta \text{sign}(\nabla_{x_i} J(x, x_t))]] \\
&= -\|s_i\| \cdot M^{-1}(x_i) \cdot u_0 - s_i^\top \cdot M^{-1}(x_i) \cdot f_i^u + \\
&\quad s_i^\top \cdot \frac{\partial}{\partial t}[\alpha \nabla_{x_i} J(x, x_t)] + s_i^\top \cdot \frac{\partial}{\partial t}[\beta \text{sign}(\nabla_{x_i} J(x, x_t))] \\
&\leq -\|s_i\| \cdot M^{-1}(x_i) \cdot u_0 + \|s_i^\top \cdot M^{-1}(x_i) \cdot f_i^u\| + \\
&\quad \|s_i^\top \cdot \frac{\partial}{\partial t}[\alpha \nabla_{x_i} J(x, x_t)]\| + \|s_i^\top \cdot \frac{\partial}{\partial t}[\beta \text{sign}(\nabla_{x_i} J(x, x_t))]\| \\
&\leq -\|s_i\| \cdot (1/\overline{M}) \cdot u_0 + \|s_i\| \cdot (1/\overline{M}) \cdot \|f_i^u\| + \\
&\quad \|s_i\| \cdot \|\frac{\partial}{\partial t}[\alpha \nabla_{x_i} J(x, x_t)]\| + \|s_i\| \cdot \|\frac{\partial}{\partial t}[\beta \text{sign}(\nabla_{x_i} J(x, x_t))]\| \\
&< -\|s_i\|[(1/\overline{M})u_0 - (1/\underline{M})\overline{f}_i - \overline{J} - \overline{J}_s] \\
&< -\epsilon \|s_i\|
\end{aligned} \tag{3.8}$$

we can guarantee that $s_i^\top \dot{s}_i < -\epsilon \|s_i\|$ for any $\epsilon > 0$, which implies that the manifold is reached in finite time. Once the sliding manifold is reached, the system remains on that manifold for all time.

Then, under ideal sliding mode, the results discussed in the preceding chapter for the “kinematic” model are recovered despite the model uncertainties in Eq. (3.1). This result is achieved thanks to the robustness properties of the sliding mode control method. If there are not known part for disturbances, this portion of the controller can be set to zero. Note also that the controller just needs the bounds on mass/inertia matrix $M(x_i)$ of the robots instead of the exact value.

The design of the sliding mode surface we considered here is little different from conventional sliding mode control problems. In classical sliding mode control problems the surface $s = 0$ is chosen such that on it the tracking error asymptotically decays to zero. Here, the surfaces $s_i = 0$ are chosen so that the system motion equation obeys certain dynamics. Even though \dot{x}_i can be viewed as the output of the system and s_i as the output error and stated that at $s_i = 0$ the output error becomes zero, there is still a difference since here s_i is not a constant surface and it can move as the agents move.

3.3 Low Pass Filter

In order to derive the above result we assumed that $\|\frac{\partial}{\partial t}[\beta \text{sign}(\nabla_{x_i} J(x, x_t))]\| \leq \bar{J}_s$, which is not the case, because the derivative of the signum function is unbounded on the switching instances. This problem could be solved by passing the switching signal through a low pass filter [14].

This idea is based on the equivalent control method [23]. The equivalent control method allows the derivation of an analytical controller assuming ideal sliding mode. Moreover, it shows that the high frequency switching controller has an “average” or an “effective” value during sliding mode. Therefore, by passing the switching signal through a low pass filter it is possible to extract that value by cutting off the high frequency component. Analogously, the $\beta \text{sign}(\nabla_{x_i} J(x, x_t))$ term must have an equivalent component and a high frequency component during sliding mode. Denote its equivalent component as $[\beta \text{sign}(\nabla_{x_i} J(x, x_t))]_{eq}$ and note that as in the sliding mode observers it can be extracted by passing $\beta \text{sign}(\nabla_{x_i} J(x, x_t))$ through an appropriate filter. Figure 3.1 shows how the low pass filter gets rid of high frequency signals.

With this in mind, we define

$$\mu \dot{z} = -z + \beta \text{sign}(\nabla_{x_i} J(x, x_t)) \quad (3.9)$$

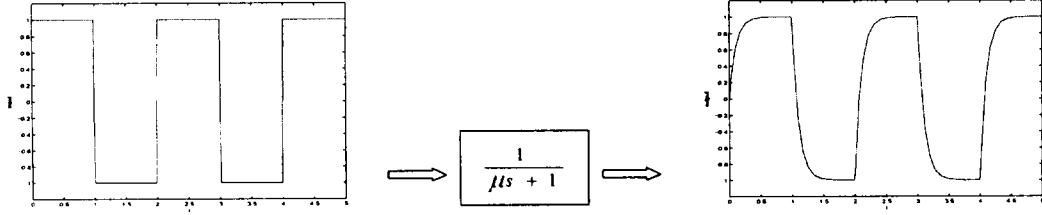


Figure 3.1: Lowpass filter ($\mu = 0.1$).

where μ is a small positive constant. In this system the high frequency switching signal $\beta \text{sign}(\nabla_{x_i} J(x, x_t))$ is the input and z is the filtered output. With proper choice of the parameter μ we have

$$z \approx [\beta \text{sign}(\nabla_{x_i} J(x, x_t))]_{eq} \quad (3.10)$$

This equation allows us to replace $\beta \text{sign}(\nabla_{x_i} J(x, x_t))$ in the sliding manifold equation in (3.2) with z . Therefore, although $\beta \text{sign}(\nabla_{x_i} J(x, x_t))$ is not differentiable, its approximation z is differentiable and can be used in the definition of the sliding manifold. One issue to notice is that μ has to be chosen properly so that the low-pass filter is able to extract the actual “average” or equivalent value of its input.

Therefore, the sliding manifold can be redefined as

$$s_{i_new} = \dot{x}_i + \alpha \nabla_{x_i} J(x, x_t) + z. \quad (3.11)$$

Since z is bounded, the method derived above could be implemented for this new sliding manifold. Moreover, we have

$$\left\| \frac{\partial}{\partial t} [\beta \text{sign}(\nabla_{x_i} J(x, x_t))]_{eq} \right\| = \|\dot{z}\| \leq \frac{2\beta}{\mu} \triangleq \bar{J}_s \quad (3.12)$$

Then, the controller in (3.6) with s_i replaced with s_{i_new}

$$u_i = -u_0 \text{sign}(s_{i_new}) + f_i^k(x_i, \dot{x}_i) \quad (3.13)$$

with gain u_0 chosen as before, guarantees the occurrence of sliding mode at the redefined manifold s_{i_new} in a finite time.

Utilizing z instead of $\beta \text{sign}(\nabla_{x_i} J(x, x_t))$ in the sliding manifold makes the algorithm implementable. This completes the development of the sliding mode controller.

However, in real applications usually it is not possible to achieve ideal sliding mode due to the use of low pass filter (because it's impossible to extract the exact value) and other unmodeled dynamics which may lead to the so called *chattering phenomenon*. Therefore, in practical implementations it may not be possible to ideally recover the exact results that could be obtained for (2.1). For example, there may be little difference between the real formation and our desired one. Nevertheless, despite the non-idealities we still would expect that the results to be recovered with reasonable error.

CHAPTER 4

RESULTS: SIMULATION

In this Chapter, we construct two specific potential functions and present the simulation results using the designed control law. We illustrate how the choice of potential function influences the application. We set $n = 2$ here, but the results should work for higher dimensions as well.

Consider the group consisting of agents with the same dynamics

$$M(x_i)\ddot{x}_i + f_i(x_i, \dot{x}_i) = u_i \quad (4.1)$$

and unity mass $M_i = 1$. Choose $\underline{M} = 0.5$, $\overline{M} = 1.5$ and let $f_i^u(x_i, \dot{x}_i) = \sin(0.2t)$ be the unknown uncertainty in the system.

Assume the target dynamics as

$$\begin{aligned} \dot{x}_{t_1} &= 0.25 \\ \dot{x}_{t_2} &= \sin(0.25t) \end{aligned}$$

We set the initial conditions of agents randomly within an area near the origin, and set the target initially at $[5, 5]$, which is located out of the agents.

4.1 Potential function with a unique minimum

For this case we chose the potential function as [9]

$$J(x, x_t) = K_T \sum_{i=1}^N \frac{1}{2} (\|x_i - x_t\|^2 - \delta_{it}^2)^2 + K_F \sum_{i=1}^{N-1} \sum_{j=i+1}^N \frac{1}{2} (\|x_i - x_j\|^2 - \delta_{ij}^2)^2 \quad (4.2)$$

where δ_{it} and δ_{ij} as defined before.

For this function, we see that

$$J_{it}(\|x_i - x_t\|) = \frac{1}{2}(\|x_i - x_t\|^2 - \delta_{it}^2)^2$$

Then, $\nabla_{(x_i - x_t)} J_{it}(\|x_i - x_t\|) = 2(\|x_i - x_t\|^2 - \delta_{it}^2)(x_i - x_t)$ where $h^{it}(\|x_i - x_t\|) = 2(\|x_i - x_t\|^2 - \delta_{it}^2)$. We can verify that $h^{it}(\|x_i - x_t\|) = 0$ if and only if $\|x_i - x_t\| = \delta_{it}$, which satisfies Assumption A2.

Moreover,

$$J_{ij}(\|x_i - x_j\|) = \frac{1}{2}(\|x_i - x_j\|^2 - \delta_{ij}^2)^2$$

Then, $\nabla_{(x_i - x_j)} J_{ij}(\|x_i - x_j\|) = 2(\|x_i - x_j\|^2 - \delta_{ij}^2)(x_i - x_j)$ where $g^{ij}(\|x_i - x_j\|) = 2(\|x_i - x_j\|^2 - \delta_{ij}^2) = 0$ if and only if $\|x_i - x_j\| = \delta_{ij}$, which satisfies Assumption B3. Since $\nabla_{x_i} J_{ij}(\|x_i - x_j\|) = 2(\|x_i - x_j\|^2 - \delta_{ij}^2)(x_i - x_j)$ and $\nabla_{x_j} J_{ij}(\|x_i - x_j\|) = -2(\|x_i - x_j\|^2 - \delta_{ij}^2)(x_i - x_j)$, Assumption B1 is satisfied too.

It also can be shown that

$$\begin{aligned} \left\| \frac{\partial}{\partial t} [\alpha \nabla_{x_i} J(x, x_t)] \right\| &\leq K_T \alpha (K_T \alpha \|x_i(0) - x_t(0)\| + K_F \sum_{j=1, j \neq i}^N (a_{ij} - b_{ij}) \|x_i(0) - x_j(0)\|) \\ &\quad + K_F K_T \alpha^2 \sum_{j=1, j \neq i}^N (\|x_i(0) - x_t(0)\| + \|x_j(0) - x_t(0)\|) \\ &\quad + K_T \alpha \beta + K_T \alpha \gamma \\ &\triangleq \bar{J} \end{aligned} \tag{4.3}$$

which is used to calculate the controller.

It is obvious that $J(x, x_t) \geq 0$ is quadratic and has a unique global minimum at $J(x, x_t) = 0$ which occurs when $\|x_i - x_t\| = \delta_{it}$ for all i and $\|x_i - x_j\| = \delta_{ij}$ for all pairs (i, j) . Therefore, in light of the discussions in the preceding chapters we would expect the formation control and the capture of the target to be exactly achieved (which is the case as seen below).

For the controller parameters, we use $\alpha = 0.01$, $\beta = 2.0$, $\bar{f}_i = 1$, and $\varepsilon = 1$. For the filter, we chose $\mu = 0.1$. With the proper choice of the agent initial conditions, we get \bar{J} and \bar{J}_s from (4.3) and (3.12), which produce the value of $u_0 = 124.5$.

In the simulations, first, Let $N = 4$, our task is to make the four agents form a diamond with the target in the mid-point. Let $\delta_{ij} = 2$ as the distance between agents, and $\delta_{it} = 1$ as the short distance between the target and agent, $\delta_{it} = \sqrt{3}$ as the long one. Formation graph is in Figure 4.1.

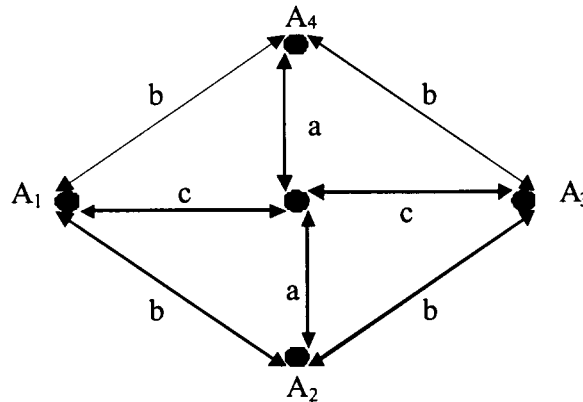


Figure 4.1: Formation graph for 4 agents and target: $a = 1$, $b = 2$, $c = \sqrt{3}$.

The simulation results can be found in Figure 4.3. In Figure 4.3 (a), the red line is the trajectory of target while the blue ones are trajectories of pursuers. We can see that after a short period, the group catches up with the target. In Figure 4.3 (b), the red lines are connections between pursuers and the green ones are those between pursuer and target. They are almost overlapped, which means the target stays at the mid-center of the diamond. Figure 4.3 (c) and 4.3 (d) show that distance between agent and target is the average value of 1 and $\sqrt{3}$, and the distance between agents

match our designed graph as well. From Figure 4.3 (e), we see that swarm maintains the formation during the whole process. Figure 4.3 (f) shows the value of potential function is minimized to 0.

Next, let's apply the controller to more agents. We consider $N = 6$ agents which are required to form an equilateral triangle formation (with any orientation) in \mathbb{R}^2 with three of the agents at the corners of the triangle and three of the agents at the middle point of the vertices. In particular, we set the lateral as 2, which result in $\delta it \in \{0.577, 1.155\}$ and $\delta ij \in \{1, 1.155, 2\}$. Figure 4.2 shows the formation graph.

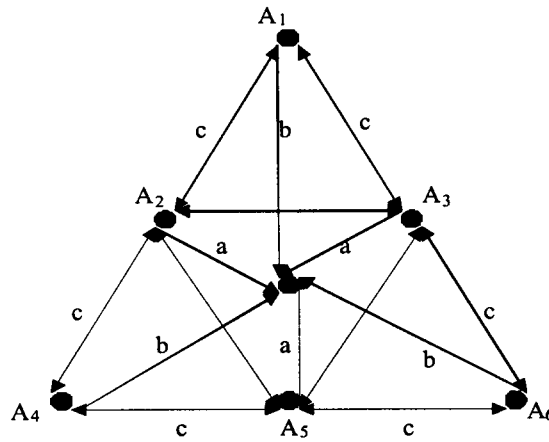


Figure 4.2: Formation graph for 6 agents and target: $a = 1/\sqrt{3}, b = 2/\sqrt{3}, c = 1$.

The simulation results can be found in Figure 4.4. From Figure 4.4 (a), we can see that after a short period, the group catches up with the target, and Figure 4.4 (b) shows the target rightly stays at the mid-center of the triangle. Figure 4.4 (c) and 4.4 (d) show that average distance between agent and target is the value of $\frac{a+b}{2}$, distance between agents is also correct. In Figure 4.4 (e), swarm formation is also maintained during the whole process. In Figure 4.3 (f), the value of potential function is almost minimized to 0.

4.2 Potential function with local minima

For this case we chose the potential function as

$$J(x, x_t) = K_T \sum_{i=1}^N \frac{1}{2} (\|x_i - x_t\|^2 - \delta_{it}^2)^2 + K_F \sum_{i=1}^{N-1} \sum_{j=i+1}^N \left[\frac{a_{ij}}{2} \|x_i - x_j\|^2 + \frac{b_{ij}c_{ij}}{2} \exp\left(-\frac{\|x_i - x_j\|^2}{c_{ij}}\right) \right] \quad (4.4)$$

where the parameters a_{ij} , b_{ij} and c_{ij} depend on the desired relative distances δ_{ij} of the individuals [13].

For this function, we can see that

$$J_{it}(\|x_i - x_t\|) = \frac{1}{2} (\|x_i - x_t\|^2 - \delta_{it}^2)^2$$

Then, $\nabla_{(x_i - x_t)} J_{it}(\|x_i - x_t\|) = 2(\|x_i - x_t\|^2 - \delta_{it}^2)(x_i - x_t)$ where $h^{it}(\|x_i - x_t\|) = 2(\|x_i - x_t\|^2 - \delta_{it}^2) = 0$ if and only if $\|x_i - x_t\| = \delta_{it}$, which satisfies Assumption A2.

Moreover,

$$J_{ij}(\|x_i - x_j\|) = \frac{a_{ij}}{2} \|x_i - x_j\|^2 + \frac{b_{ij}c_{ij}}{2} \exp\left(-\frac{\|x_i - x_j\|^2}{c_{ij}}\right)$$

Here $\frac{a_{ij}}{2} \|x_i - x_j\|^2$ is the attraction part between agents and $\frac{b_{ij}c_{ij}}{2} \exp\left(-\frac{\|x_i - x_j\|^2}{c_{ij}}\right)$ is the repulsion part. We see that, $\nabla_{(x_i - x_j)} J_{ij}(\|x_i - x_j\|) = [a_{ij} - b_{ij} \exp\left(-\frac{\|x_i - x_j\|^2}{c_{ij}}\right)](x_i - x_j)$ where $g^{ij}(\|x_i - x_j\|) = a_{ij} - b_{ij} \exp\left(-\frac{\|x_i - x_j\|^2}{c_{ij}}\right)$. We can verify that $g^{ij}(\|x_i - x_j\|) = 0$ if and only if $\|x_i - x_j\| = \delta_{ij}$, which satisfies Assumption B3. The distance $\delta_{ij} = \sqrt{c_{ij} \ln(b_{ij}/a_{ij})}$ is the distance at which the attraction and repulsion balance [10, 11], which also defines the distance between the agents in the desired formation. We can further verify it satisfies Assumption B1 too.

It also can be shown with certain manipulation that

$$\begin{aligned}
\left\| \frac{\partial}{\partial t} [\alpha \nabla_{x_i} J(x, x_t)] \right\| &\leq (K_T + (M-1)K_F)\alpha(K_T\alpha\|x_i(0) - x_t(0)\| + \\
&\quad K_F \sum_{j=1, j \neq i}^M (a_{ij} - b_{ij})\|x_i(0) - x_j(0)\|) + \\
&\quad K_F\alpha \sum_{j=1, j \neq i}^M (K_T\alpha\|x_j(0) - x_t(0)\| + \\
&\quad K_F \sum_{j=1, j \neq i}^M (a_{ij} - b_{ij})\|x_i(0) - x_j(0)\|) + \\
&\quad K_T\alpha\beta + K_T\alpha\gamma + K_F\alpha\beta p(M-1) \\
&\triangleq \bar{J}
\end{aligned} \tag{4.5}$$

where p is some constant.

We notice that J has a global minimum at $J(x, x_t) = 0$ which occurs when $\|x_i - x_t\| = \delta_{it}$ for all i and $\|x_i - x_j\| = \delta_{ij}$ for all pairs (i, j) . But there may be other minima because second item is not quadratic.

In the simulations, we apply the controller to both 4-agent case and 6-agent case, obtaining the controller parameter with the same procedure in last section.

The simulation results for $N = 4$ can be found in Figure 4.5. In Figure 4.5 (a) and (b), we see that after a short period, the group follows the target, but the formation is not what we want. The target even escapes from the pursuing group. Figure 4.5 (e) shows formation is changing from time to time. Although J is also minimized to 0 in Figure 4.5 (f), the system is obviously locked at a local minimum, which corresponds to an undesired configuration.

The simulation results for $N = 6$ can be found in Figure 4.6. From Figure 4.6 (a) and (b), we see that after a short period, the same thing happens. The group follows the target, but the formation is messed up, either. The system is converging to an undesired configuration.

Based on the extended discussion in Chapter 2, we shall redefine J to make sure $h^{it}(\|y\|) \geq 0$ or $h^{it}(\|y\|) \leq 0$ for all y so that we can at least guarantee the agents will “surround” or “enclose” the target.

$$J(x, x_t) = K_T \sum_{i=1}^N \frac{1}{3} [(\|x_i - x_t\|^2 - \delta_{it}^2)^3 + \delta_{it}^6] + K_F \sum_{i=1}^{N-1} \sum_{j=i+1}^N \left[\frac{a_{ij}}{2} \|x_i - x_j\|^2 + \frac{b_{ij}c_{ij}}{2} \exp\left(-\frac{\|x_i - x_j\|^2}{c_{ij}}\right) \right] \quad (4.6)$$

For this function, we can see that

$$J_{it}(\|x_i - x_t\|) = \frac{1}{3} (\|x_i - x_t\|^2 - \delta_{it}^2)^3$$

where $h^{it}(\|x_i - x_t\|) = 2(\|x_i - x_t\|^2 - \delta_{it}^2)^2$. We can verify that $h^{it}(\|x_i - x_t\|) > 0$ for all $\|x_i - x_t\|$ except $\|x_i - x_t\| = \delta_{it}$. Therefore, we would expect that the agents would enclose the target, regardless of initial conditions.

The simulation results for $N = 4$ can be found in Figure 4.7. From Figure 4.7 (a) and (b), we see that after a short period, the group follows and encloses the target.

The simulation results for $N = 6$ can be found in Figure 4.8. From Figure 4.8 (a) and (b), we see that performance is better.

It is well known that, practically, potential functions may have many local minima. Therefore, usually when potential functions are used for coordinated tracking in a formation it is impossible to drive with global results, but only local results can be obtained. This problem has been observed in many other practical implementations [17]. In particular, for the formation control problem we are considering there may be several different families of minima. The first family is at the desired formation and the other families occur when the agents are at points at which the attraction and repulsion forces balance. This requires careful consideration and more research.

The beauty of the sliding mode control method discussed here is that it is independent on the potential function chosen as long as the boundedness assumptions are satisfied. Moreover, the objectives are achieved despite the model uncertainties.

4.3 Formation switching

While a team of agents is searching an environment, it may be beneficial for the team to assume a structured formation. However, once the team has detected the disturbance, their formation may no longer be ideally suited to the task at hand. Therefore, formation reconfiguration becomes another interesting topic besides formation maintenance. Change in team-strategy and formation goals, loss or damage of an agent, and emergence of an external threat are all situations which may necessitate formation reconfiguration. In our context, there are two different approaches — switch the potential function that defines the formation on particular instances or define the potential function as a time-dependent function. In this section, we present two simulation results for each of them.

First, we want the swarm switch from a diamond to a triangle where three agents stay at one lateral and the last one at the opposite vertices. The target is still enclosed in the center of swarm. From Figure 4.9, we see that the formation switches successfully and is maintained afterwards. Second, we want it keep the diamond shape but changing size from time to time. We set the value of lateral as a time-varying function. Figure 4.10 shows that the swarm performance achieves our goal.

For two cases here we use the potential function in Section 1 and the same control law. The work beyond system verification through simulation that must be examined is to theoretically analyze the system. This may prove difficult as the formation is time-varying, creating discontinuities in the potential functions. Steps must be taken

to theoretically prove the stability of the dynamic formation. This requires careful consideration and can be part of the future research.

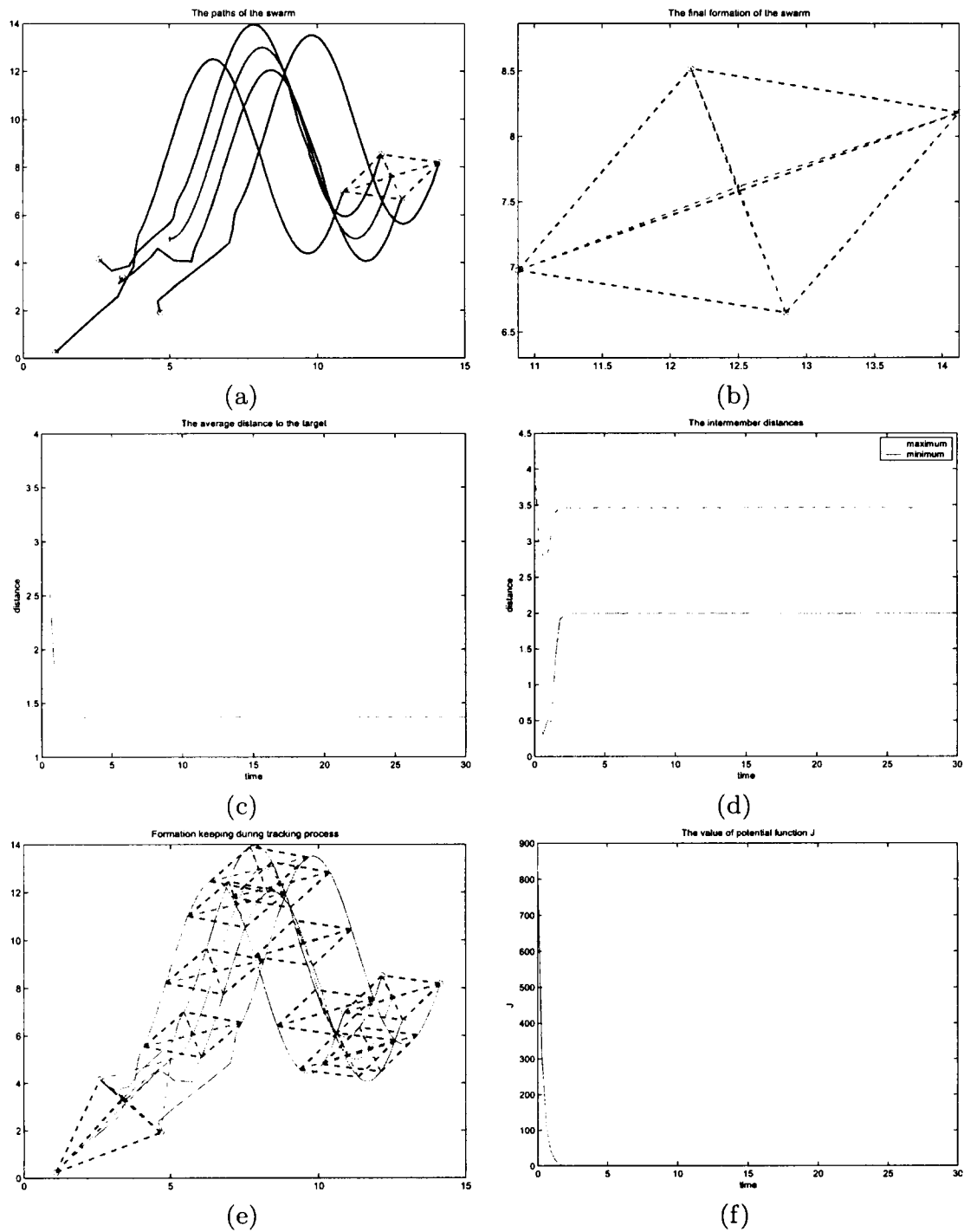


Figure 4.3: Swarm performance for $N = 4$ using potential function with unique minimum. (a) The paths of the swarm members. (b) Zoomed out final position of the swarm. (c) Distance between agent and target. (d) Distance between agents. (e) Formation keeping. (f) Potential function.

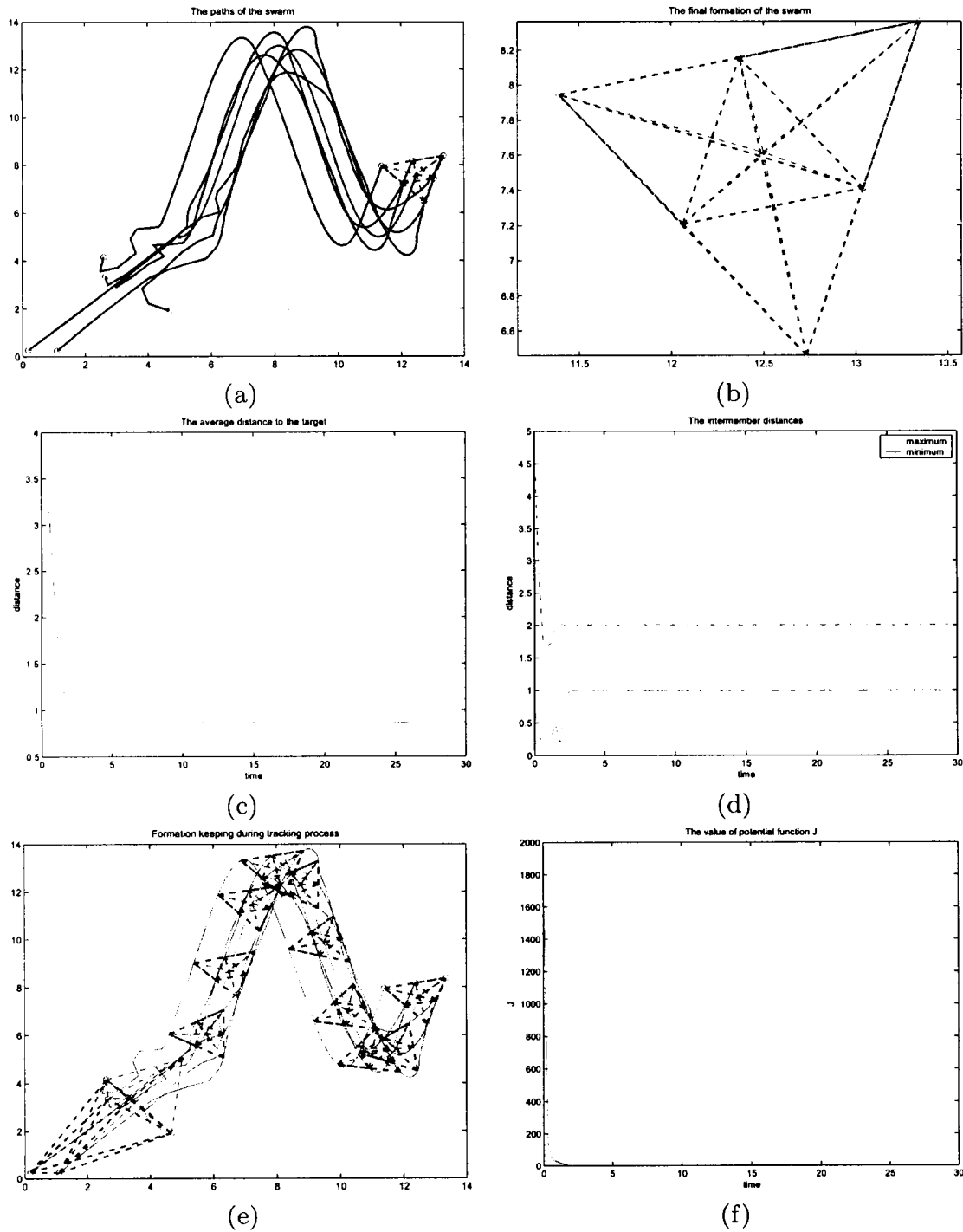


Figure 4.4: Swarm performance for $N = 6$ using potential function with unique minimum. (a) The paths of the swarm members. (b) Zoomed out final position of the swarm. (c) Distance between agent and target. (d) Distance between agents. (e) Formation keeping. (f) Potential function.

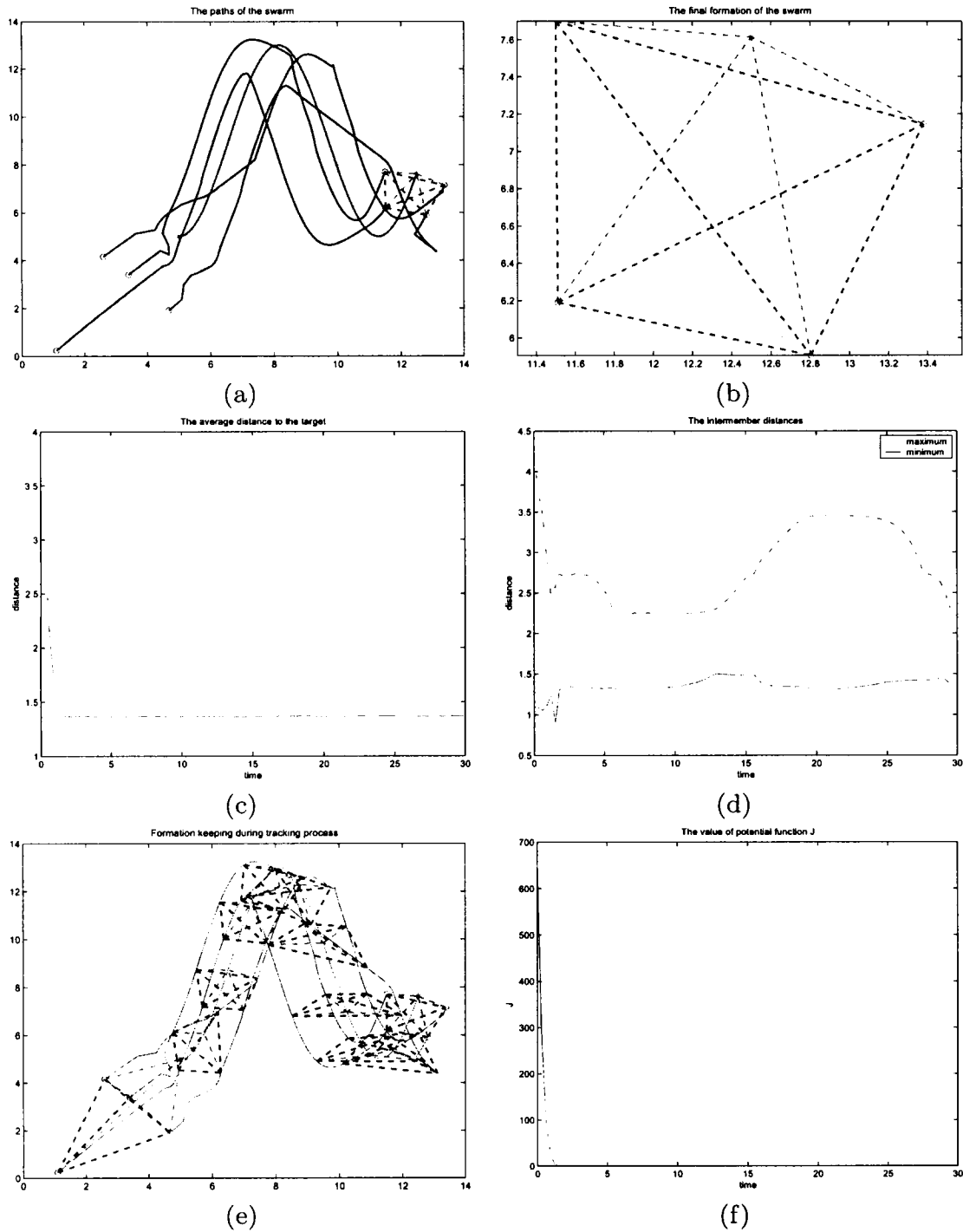


Figure 4.5: Swarm performance for $N = 4$ using potential function with local minima. (a) The paths of the swarm members. (b) Zoomed out final position of the swarm. (c) Distance between agent and target. (d) Distance between agents. (e) Formation keeping. (f) Potential function.

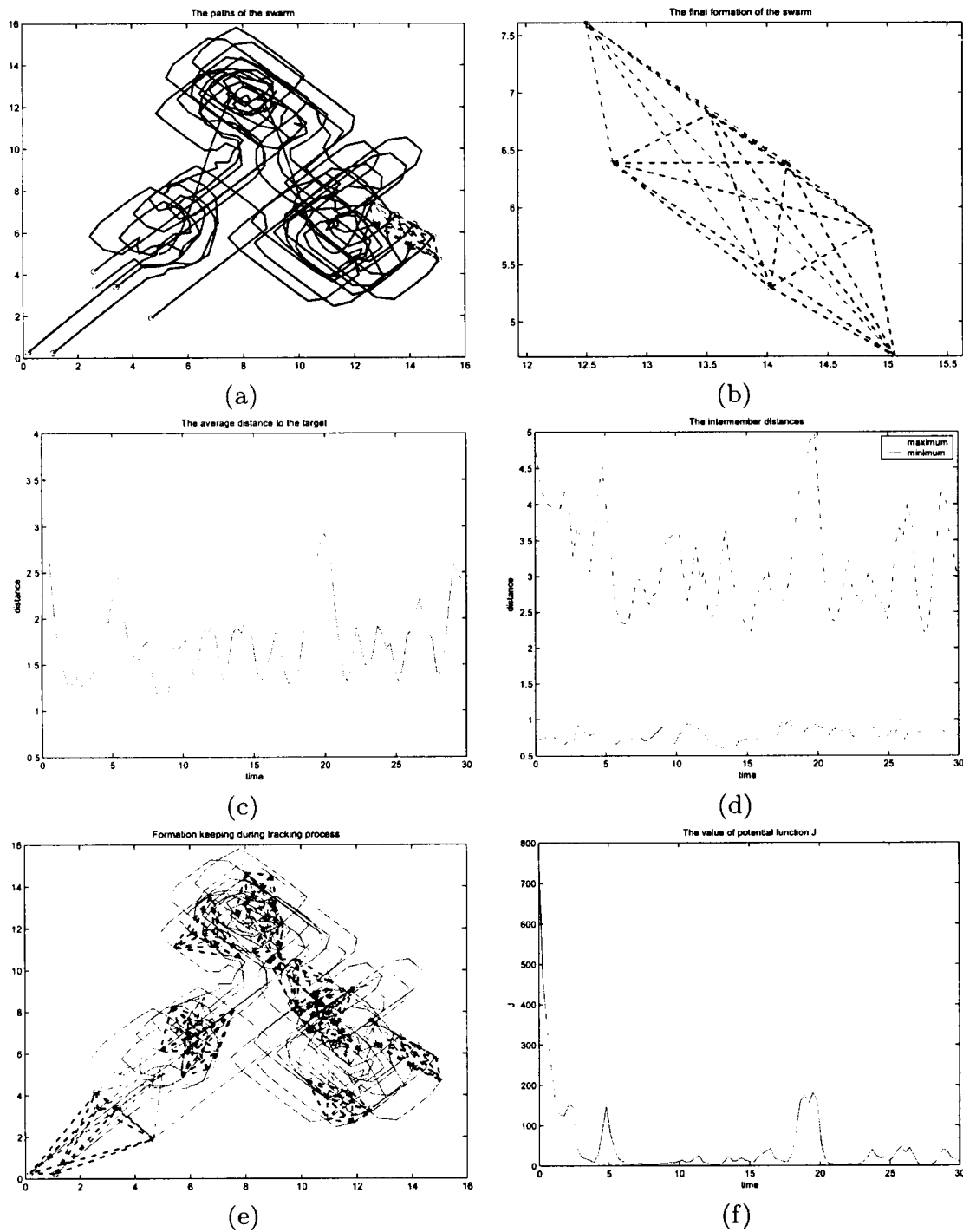


Figure 4.6: Swarm performance for $N = 6$ using potential function with local minima. (a) The paths of the swarm members. (b) Zoomed out final position of the swarm. (c) Distance between agent and target. (d) Distance between agents. (e) Formation keeping. (f) Potential function.

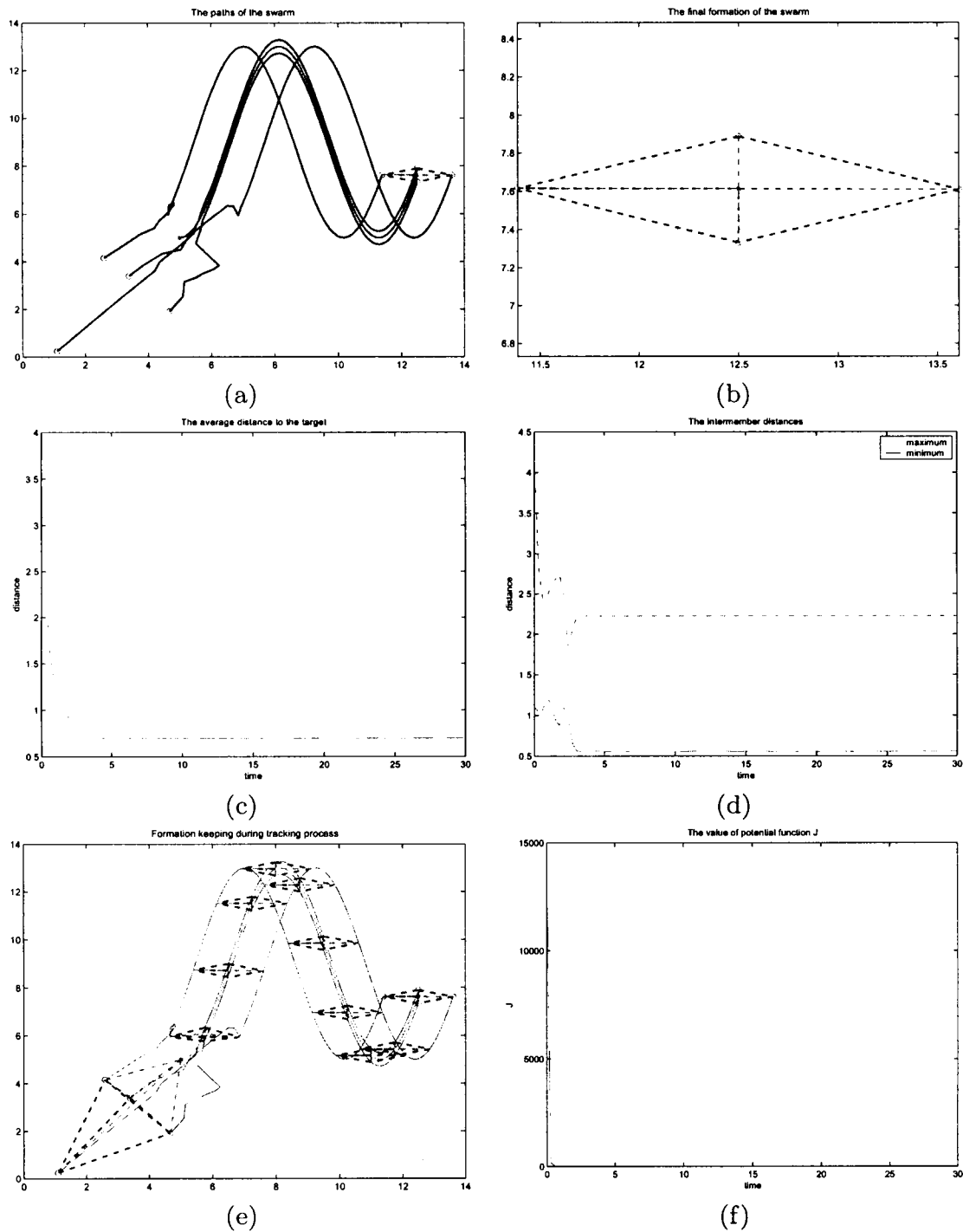


Figure 4.7: Swarm performance for $N = 4$ using improved potential function with local minima. (a) The paths of the swarm members. (b) Zoomed out final position of the swarm. (c) Distance between agent and target. (d) Distance between agents. (e) Formation keeping. (f) Potential function.

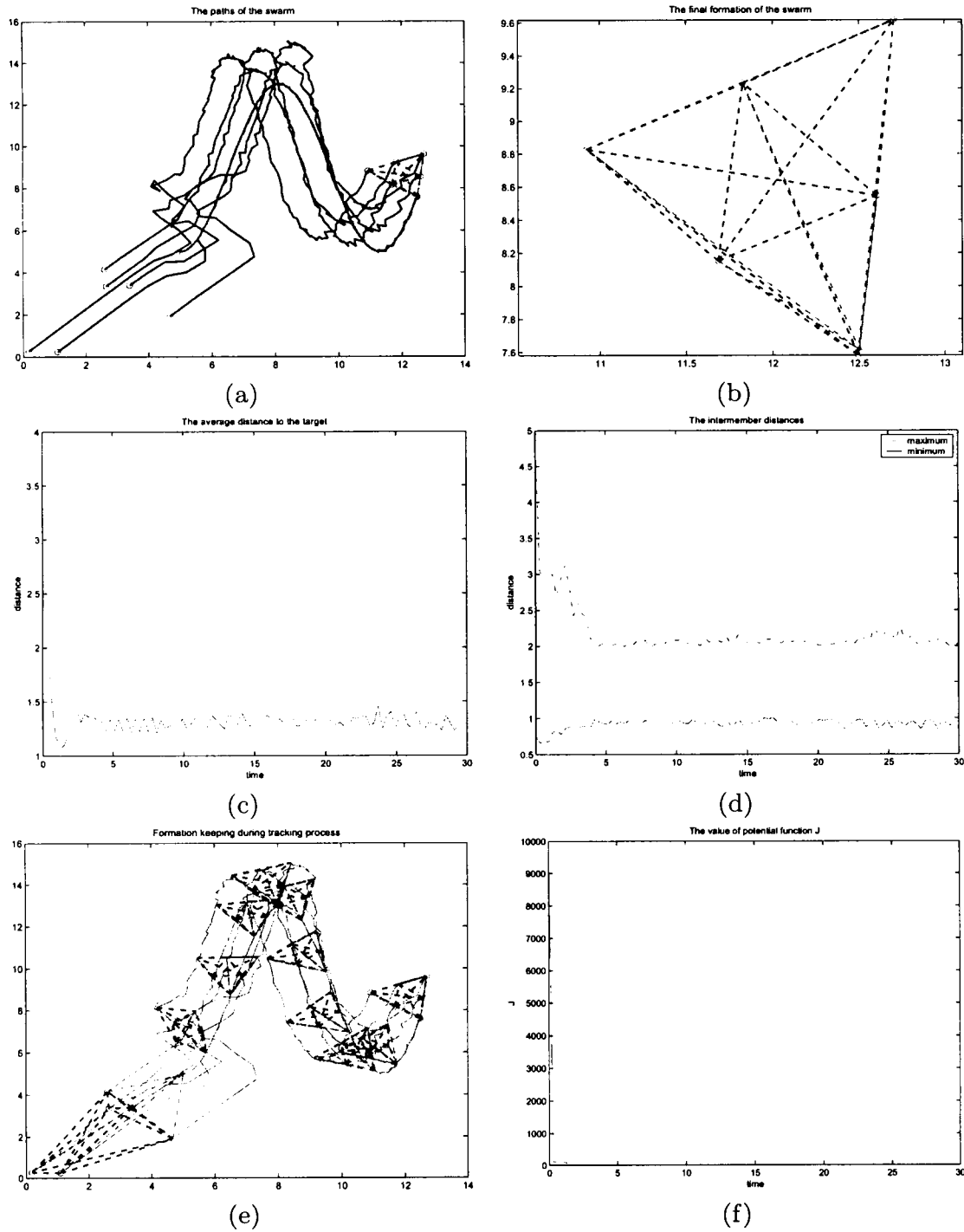


Figure 4.8: Swarm performance for $N = 6$ using improved potential function with local minima. (a) The paths of the swarm members. (b) Zoomed out final position of the swarm. (c) Distance between agent and target. (d) Distance between agents. (e) Formation keeping. (f) Potential function.

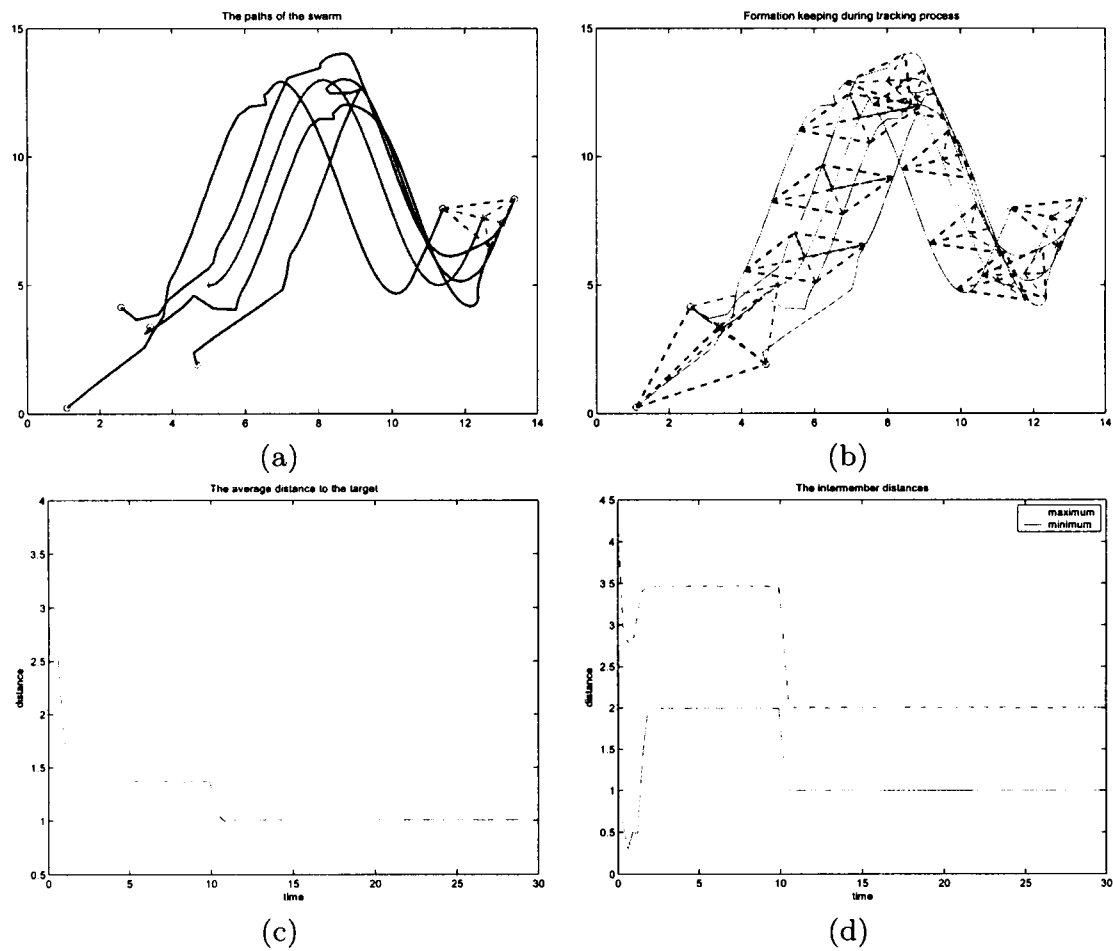


Figure 4.9: Swarm performance ($N = 4$) of formation switching at $t = 10$. (a) The paths of the swarm members. (b) Formation changing. (c) Distance between agent and target. (d) Distance between agents.

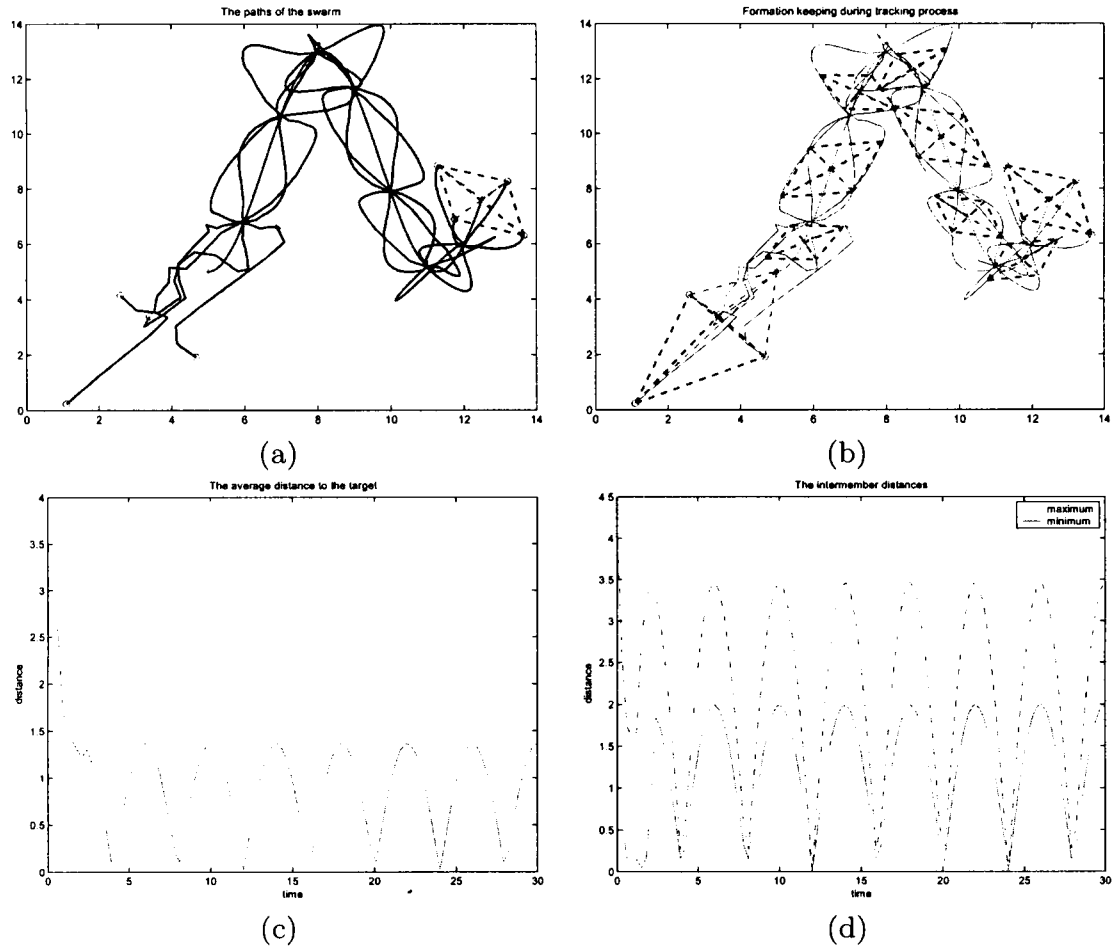


Figure 4.10: Swarm performance ($N = 4$) of time-varying formation. (a) The paths of the swarm members. (b) Formation changing. (c) Distance between agent and target. (d) Distance between agents.

CHAPTER 5

CONCLUSIONS

We presented a procedure to implement coordinated tracking problem using artificial potential and sliding mode control. Cyclic architecture based strategy makes swarm maintain a more robust formation than other strategies such as leader-follower structure.

In Chapter 2, first of all, a potential function with a general form for individual was defined to encode the overall tasks. It includes the tracking term and the formation term so that each agent take care of both tasks and will react if any given agent cannot keep up with the target. Then, a basic controller was designed for agents in “kinematic” model. The stability proof obtained is based on general potential function and conclusion was made that tracking and formation were both achieved. We also showed that potential function can be modified to make group at least enclose the target if the potential function has multi-minima. The results we got in this chapter serve as guidelines for next step designing.

In Chapter 3, we defined a sliding surface for agents in general dynamic model. A controller was designed using Lyapunov analysis to enforce occurrence of sliding mode on the assigned surface. As a difference from usual sliding surfaces, the sliding manifold considered here contains a switching term with unbounded first derivative. This difficulty was overcome by redefining the manifold and replacing the switching term with its smooth steady state equivalent. The procedure is general and not

limited only to the models here, but can be applied also to other similar models or contexts.

Finally, simulation results for 4-agent tracking in diamond formation and 6-agent tracking in triangle formation were shown in Chapter 4. The swarm tracked the target and maintained a formation as a consequence of following the designed control law. Given two specific potential function, we compared the results and showed how to improve when system was locked in local minimum. We also give out some simulation results for formation switching cases.

Future research may focus on theoretical analysis for formation reconfiguration (time varying or dynamic formations) as well as putting bounds on control signal for implementation purposes. Another promising work is to apply the procedure to vehicle modeled as unicycle. It has non-holonomic constraints and we see it on many robots.

BIBLIOGRAPHY

- [1] W. Kang, N. Xi, and A. Sparks, "Formation control of autonomous agents in 3d workspace," in *Proc. of the 2000 IEEE International Conference on Robotics and Automation*, (San Francisco, CA), April 2000.
- [2] T. Balch and R. C. Arkin, "Behavior-based formation control for multirobot teams," *IEEE Transactions on Robotics and Automation*, vol. 14, pp. 926–939, December 1998.
- [3] J. P. Desai, J. Ostrowski, and V. Kumar, "Controlling formations of multiple mobile robots," in *Proc. 1998 IEEE Int. Conf. Robotics and Automation*, (Leuven, Belgium), pp. 2864–2869, May 1998.
- [4] J. P. Desai, J. Ostrowski, and V. Kumar, "Modeling and control of formations of nonholonomic mobile robots," in *IEEE Trans. on. Robotics and Automation*, vol. 17, pp. 905–908, December 2001.
- [5] R. Olfati-Saber and R. M. Murray, "Distributed cooperative control of multiple vehicle formations using structural potential functions," in *Proc. of the IFAC World Congress*, (Barcelona, Spain), June 2002.
- [6] J. R. Lawton, B. J. Young, and R. W. Beard, "A decentralized approach to elementary formation maneuvers," in *Proc. IEEE International Conf. on Robotics and Automation*, (San Francisco, CA), pp. 2728–2743, April 2000.
- [7] N. E. Leonard and E. Fiorelli, "Virtual leaders, artificial potentials and coordinated control of groups," in *Proc. 40th IEEE Conf. Decision and Control*, (Orlando, FL), pp. 2968–2973, December 2001.
- [8] P. Ögren, E. Fiorelli, and N. E. Leonard, "Cooperative control of mobile sensor networks: Adaptive gradient climbing in a distributed environment," *IEEE Transaction on Automatic Control*, vol. 49, pp. 1292–1302, August 2004.
- [9] M. Egerstedt and X. Hu, "Formation constrained multi-agent control," *IEEE Transaction on Robotics and Automation*, vol. 17, pp. 947–951, December 2001.
- [10] V. Gazi and K. M. Passino, "A class of attraction/repulsion functions for stable swarm aggregations," *International Journal of Control*, vol. 77, pp. 1567–1579, December 2004.

- [11] V. Gazi and K. M. Passino, "Stability analysis of swarms," *IEEE Transactions on Automatic Control*, vol. 48, pp. 692–697, April 2003.
- [12] V. Gazi and K. M. Passino, "Stability analysis of social foraging swarms," *IEEE Transactions on Systems, Man, and Cybernetics: Part B*, vol. 34, pp. 539–557, February 2004.
- [13] V. Gazi, "Swarm aggregations using artificial potentials and sliding mode control," *IEEE Transactions on Robotics*, vol. 21, pp. 1208–1214, December 2005.
- [14] V. Gazi and R. Ordóñez, "Target tracking using artificial potentials and sliding mode control," in *Proc. American Control Conference*, (Boston, MA), pp. 5588–5593, June-July 2004.
- [15] D. P. Scharf, F. Y. Hadaegh, and S. R. Ploen, "A survey of spacecraft formation flying guidance and control (part ii): Control," *International Journal of Control*, vol. 71, no. 6, pp. 1051–1067, 1998.
- [16] J. H. Reif and H. Wang, "Social potential fields: A distributed behavioral control for autonomous robots," *Robotics and Autonomous Systems*, vol. 27, no. 3, pp. 171–194, 1999.
- [17] E. Rimon and D. E. Koditschek, "Exact robot navigation using artificial potential functions," *IEEE Transaction on Robotics and Automation*, vol. 8, pp. 501–518, October 1992.
- [18] H. Yamaguchi, "A cooperative hunting behavior by mobile-robot troops," *The International Journal of Robotics Research*, vol. 18, pp. 931–940, September 1999.
- [19] D. H. Kim, H. O. Wang, G. Ye, and S. Shin, "Decentralized control of autonomous swarm systems using artificial potential functions: Analytical design guidelines," in *IEEE Conference on Decision and Control*, December 2004.
- [20] J. Guldner and V. Utkin, "Sliding mode control for an obstacle avoidance strategy based on an harmonic potential field," in *Proc. Of Conf. Decision Contr.*, (San Antonio, Texa), pp. 424–429, December 1993.
- [21] J. Guldner and V. Utkin, "Sliding mode control for gradient tracking and robot navigation using artificial potential fields," *IEEE Trans. On Robotics and Automation*, vol. 11, no. 2, pp. 247–254, 1995.
- [22] J. Yao, R. Ordóñez, and V. Gazi, "Swarming tracking using using artificial potentials and sliding mode control," in *Submitted to the Conference Decision and Control*, 2006.
- [23] I. Haskara, Ü. Özgüner, and V. I. Utkin, "On sliding mode observers via equivalent control approach," *International Journal of Control*, vol. 71, no. 6, pp. 1051–1067, 1998.

002588788